A Thesis

On

Structural and dielectric investigations of nano dispersed poly (vinylidene fluoride) (PVDF) composites

Submitted in the partial fulfillment of requirement for the degree of

Master of Technology

in

Material Science and Engineering

by

Akash Katoch

(60702002)

Under the supervision of

Dr. K.K. Raina

School of Physics and Materials science

Thapar University, Patiala, (Punjab)

June-2009

Dedicated
to
My Loving Parents

Certificate

This is to certify that the thesis entitled **"Structural and dielectric investigations of nano dispersed poly (vinylidenefluoried) (PVDF) composites."** submitted by **Akash Katoch** in the partial fulfilment of the requirement for the award of the degree of **M.Tech.** in **Materials Science and Engineering** from the School of Physics and Materials Sciences, Thapar University, Patiala, is a record of candidate's own work carried out by her under my supervision and guidance. The experimental matter embodied in this report has not been submitted in part or full to any other university or institute for the award of any degree.

Date:
Place:

Dr. K.K. Raina
Deputy Director,
Dean, Faculty
Dean, RPG
Thapar University, Patiala

Countersigned by:

Dr. O.P. Pandey
Prof. and Head,
Thapar University,
Patiala, Punjab.

29/7

Dr. R.K. Sharma
Dean, Academic Affairs
Thapar University,
Patiala, Punjab.

Acknowledgment

I am submitting my thesis report and this work would not have been accomplished without the support, help and guidance of a large number of people. I express my deep gratitude and respect to my supervisor **Dr. K. K. Raina, Professor and Deputy Director, School of Physics and Material Science**, for his keen interest, strong motivation and constant encouragement during the course of the work. I thank him from the bottom of my heart for introducing me to the area of electroceramics. I thank him for his great patience, constructive criticism and myriad useful suggestions apart from invaluable guidance to me.

I am grateful to **Dr. O.P. Pandey, Professor and Head, School of Physics and Materials Science** for his encouragement and execution of thesis work.

I am extremely thankful to **Dr. M L Singla, Scientist "G"** in CSIO, Chandigarh, without whom the work would not have been possible.

I would also like to thank **Dr. Kulvir Singh, Assistant Professor and PG Incharge, School of Physics and Materials Science** for his constant guidance and encouragement.

I am also thankful to **Mr. Pankaj Kumar** and all the faculty members of School of Physics and Materials Sciences for their constructive suggestions at different stages of this work.

It gives me immense pleasure to express my special thanks to **Mr. Ravi Shukla** (Ph.D. scholar), who always took keen interest in guiding me during my work. I wish to express my warm and sincere thanks to **Miss Neeraj Sharma** (Ph.D. scholar) and my colleagues **Preeti Makkar** and **Ranvir Panwar** for their support and their timely help and valuable discussions.

I owe my sincere thanks to all the staff members of School of Physics and Materials Science for their support and encouragement. Last but not the least; I would like to thank my parents for their moral support that kept my spirit up during the endeavor.

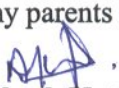

Akash Katoch

Chapter 1
Introduction

One goal of today's technology is the miniaturization of the electronic, actuating, sensing, and optical devices and their components; hence, nanotechnology attracts much attention from the worlds of the science and industry. Nanotechnology offers new design, characterization, production, and application of systems, devices and materials at the nanometer scale.

Nowadays polymers play a very important role in numerous fields of everyday life due to their advantages over conventional materials (e.g. wood, clay, metals) such as lightness, resistance to corrosion, ease of processing, and low cost production. Further improvement of their performance, including composite fabrication, still remains under intensive investigation. The altering and enhancement of the polymer's properties can occur through doping with various nano-fillers such as metals, semiconductors, organic and inorganic particles and fibres, as well as carbon structures and ceramics[2-5]. Such additives are used in polymers for a variety of reasons, for example: improved processing, density control, optical effects, thermal conductivity, control of the thermal expansion, electrical properties that enable charge dissipation or electromagnetic interference shielding, magnetic properties, flame resistance, and improved mechanical properties, such as hardness, elasticity, and wear resistance .

Conventional fibres made from materials such as alumina, glass, boron, silicon carbide and carbon have been used as fillers in composites. Compared to those fibres, carbon nanotubes (CNTs) have many superior properties such as low-weight, very high aspect ratio, high electrical conductivity, elastic moduli in the PTa range, and much higher fracture strain. These outstanding properties of CNTs make them an attractive candidate for making advanced composite materials with multifunctional features. However, the preparation of satisfactory composites is still a great challenge. An analysis of the registered patents regarding the fabrication of polymer composites containing carbon nanotubes reveals that several fundamental processing challenges such as purification, dispersion, alignment and adhesion of nanotubes and the limitations in interfacial load transfer must be overcome [6]. In addition, another major obstacle to use CNTs as fillers is the high expenses, though it can be only a matter of time to produce CNTs at low cost Nanocomposites consisting of silicate nanoparticles in a polymer matrix have attracted

considerable technological and scientific interests in recent years due to their outstanding physical and mechanical properties, such as high strength and stiffness, flame retardation, and gas permeability barrier. The industrial use of silica is widespread from micro electronics technology. The excellent electrical and dielectric properties of silica are extensively used in dynamic random access memory and field-effect transistors (Kingon et al., 2000; Wilk e t al., 2001) [7-8]. Nanocrystalline silica has been incorporated into a variety of conjugated polymers to obtain better physical properties [9]. Additionally polymer-oxide nanocomposites are favored because they require lower processing temperatures while providing the high dielectric constant of oxides as well as overcoming the fragility of pure oxide films.

1. Polyvinylidene fluoride:

Poly(vinylidene)fluoride or **PVDF** (CH_2-CF_2) is a highly non-reactive and pure thermoplastic fluoropolymer. It is also known as **KYNAR**, **HYLAR** or **SYGEF**. PVDF has been known since 1969 and is a material with relatively high piezoelectric constants. Poly(vinylidene fluoride) (PVDF) is one of the semi crystalline polymers with at least four crystalline forms referred to as α, β, γ and δ phase, among which the β phase has gained substantial importance due to its advantageous pyro- and piezoelectric properties [9].

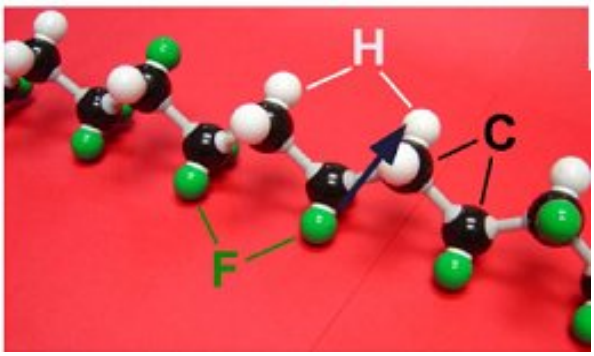

Figure 1.1: Chemical structure of PVDF polymer.

There are at least four crystalline structures which are stable at room temperature and three of these phases have net dipolar moments, the β-phase being dominant[9]. Conversion from the non-polar crystalline structure to a polar form can be induced by uniaxially or biaxially mechanical stretching, or by high temperature annealing. In addition to these phase changes, it is also possible to create changes in the orientation of the crystal moment by application of large electrical fields.

1.1 Microscopic detail of PVDF

PVDF crystallizes from the melt into spherulitic structures. The volume fraction of crystalline material is typically about 50%, depending on thermal history. Most of the uncrystallised molecules are in a meta stable liquid phase. The glass transition temperature for this liquid phase is around -50°C. The spherulites consist of stacks.

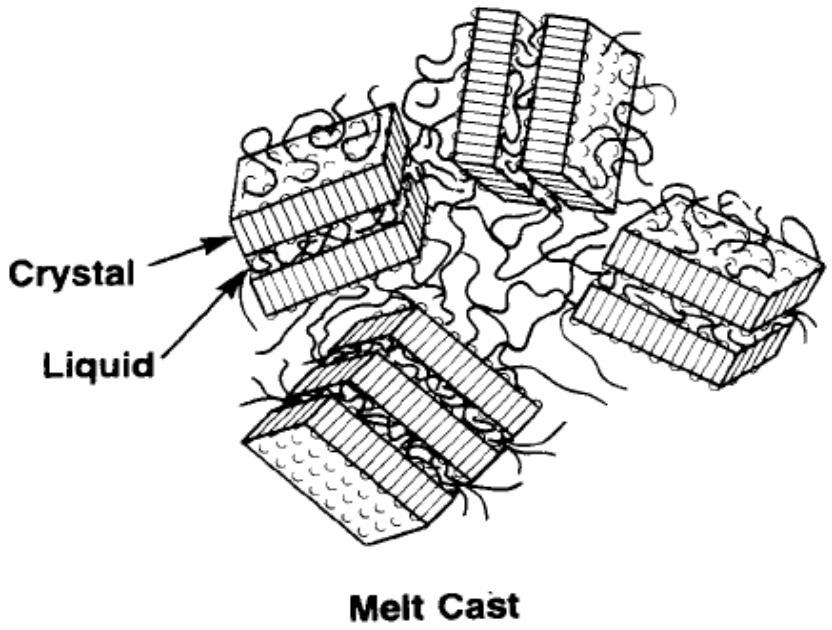

Figure1.2 Schematic picture showing random stacks of liquid and crystal lamellae in a sample of PVDF grown from the melt. Stacks are more densely packed and more irregular in size and shape in a real film.

Lamellae those grow outward from a common centre during crystallization. These lamellae are typically 10-20 nm thick, depending on crystallization conditions. The molecular chains are approximately normal to the large lamellae surfaces and to the radii of the spherulites[9]. Much of the liquid material is probably located between the crystal lamellae; typical region is shown schematically in the top part of Figure 1.2. It consists of parallel layers of alternating crystal and liquid material, each layer of the order of 10-20 nm thick[11].

Since the molecular lengths are of the order of 100 times the lamellae thicknesses, each molecule may pass many times through one or more of the crystal layers and is free to assume flexible and irregular configurations in the liquid layers.

In the crystal phase, certain regular molecular conformations are energetically favoured for crystal packing. Viewed down the molecular chain, four such conformations are shown in Figure1.3**.**

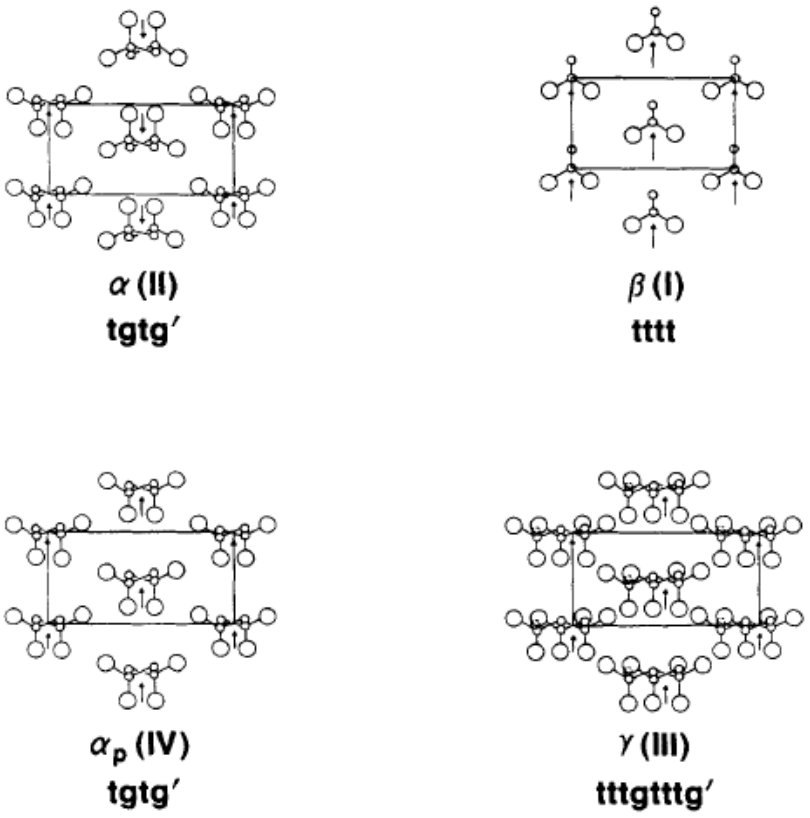

Figure1.3 Projection of crystal structures of PVDF viewed along the molecular axes. Larger circles represent fluorine, smaller circles represent carbon, and hydrogen's are not shown.

All four crystal structures are long lived (whether stable or metastable) at room temperature and three have polar unit cells. That is, a crystal of polar alpha, beta, or gamma phase has a net dipole moment. Crystal phase transformations can occur through mechanical stretching, high temperature annealing or application of electric fields. In addition to phase changes, changes in orientation of the crystal moment can occur in large electric fields. The field induced changes in orientation and phase occur by rotations about carbon-carbon bonds, or by rotation of molecular segments about their long axes or both. The driving force for these changes is the decrease in the applied electric field molecular dipole interaction energy which is extremely large. A typical molecular segment in the crystal has a dipole moment of roughly 2×10^{28} Cm. The energy of interaction between it and a field of 10^8 V/m is several times the thermal energy at room temperature and comparable to the energies needed to rotate molecules in the crystal phase. Thus PVDF is truly ferroelectric, but with the polar alignment caused by Vander Waals forces rather

than dipole-dipole forces and with a Curie transition (between ferro- and paraelectric states) temperature above the crystal melting range of 170-200 ºC[11].

Dipolar alignment occurs by rotation of molecular segments within the crystal phase, about the molecular chain axis (the 1' axis in Figure 1.4**).** Crystal poling, then, is best done when the molecular segments are normal to the poling field, i.e. in the plane of the film.

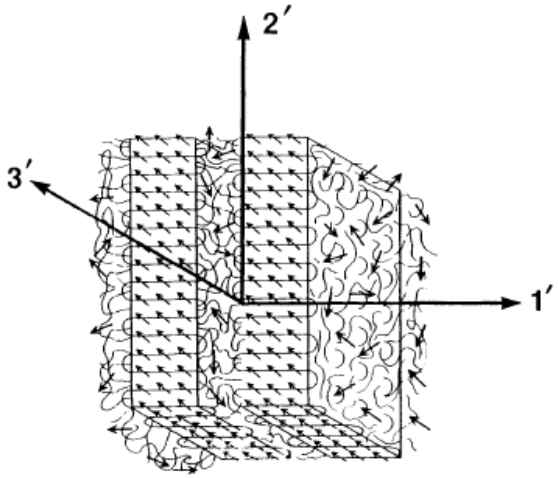

Figure1.4 Schematic picture of a crystal-liquid stack showing the chain and dipole directions in the crystals.

1.2 Carbon Nanotubes

The carbon nanotubes (CNT) were discovered in 1976 [12] when Endo synthesized vapour-grown carbon fibres. In 1991, Sumio Iijima, a researcher at the NEC Laboratory in Japan, observed that these fibers were hollow. The diameter of a nanotube is on the order of one nanometer, many times smaller than the width of a human hair, but up to several microns long. CNTs come in two principal forms, single-walled carbon nanotubes (SWCNT) and multi-walled (MWCNT). Carbon nanotubes (CNT) are molecular scale tubes of graphitic carbon with outstanding properties. CNTs are among the stiffest and strongest materials known, and have remarkable electronic properties and many other unique characteristics. For these reasons they have attracted lots of academic and industrial interest.

1.2.2 Carbon Nanotubes Structure

CNTs are considered to be a rolled-up graphene sheet that forms long concentric cylinders .The binding in carbon nanotubes is sp^2 with each carbon atom joined to three neighbour carbon atoms, as in graphite. Graphite has a sheet like structure where carbon atoms all lie at the corners

of hexagons in a plane and are only weakly bonded to the graphite sheets above and below with a interlayer distance of 0.34 nm. Carbon nanotubes can be considered as rolled-up graphene sheets (graphene is the term to namely armchair, zigzag [13].

1.2.2.1 Types of CNTs:

1.2.2.1.1 Single wall carbon nanotubes (SWNTs) are hollow single cylinders of a grapheme sheet, which are defined by their diameter and their chirality. The diameter of SWNTs varies from 0.5 to 5 nm. Depending on the chirality SWNTs may either be metallic or semiconducting [13].

1.2.2.1.2 Multiwall carbon nanotubes (MWNTs) are a group of concentric SWNTs (Figure 1.10) often capped at both ends, with diameters in the range from several nano meters up to 200 nm. These concentric nanotubes are held together by Vander Waals bonding. MWNTs form complex systems with different wall numbers, structures, and properties and additional features such as: tips, internal closures within the central part of the tube, forming a so called “bamboo” structure and even an angle Y-junction formation of MWNTs [13].

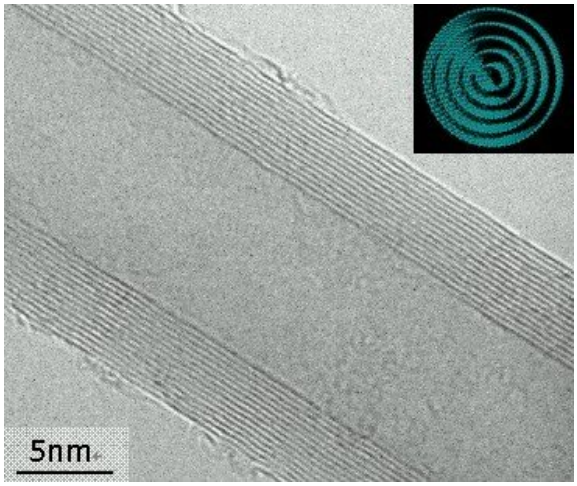

Figure 1.5 High resolution transmission electron microscope images of MWNTs.

The effective utilization of CNTs in composite applications depends strongly on the ability to disperse them homogeneously throughout the matrix. Chemical modifications have become an important issue due to the poor solubility of the CNTs in almost any solvent. Therefore, various functionalization strategies of the surface of the carbon nanotubes have been developed

Chemical modification of CNTs ensures good dispersion of nanotubes in a medium, and enhances the interfacial bonding between filler and matrix, which is crucial to achieve a load transfer across the CNT/matrix interface. This is a necessary condition for the improvement of the mechanical properties of such composites and better stability of the systems. As a result of the presence of CNTs in composite, improvements of the properties of the matrix material such as: enhanced mechanical performance high electrical conductivity, better thermal conductivity, and anisotropic optical properties are observed [14-15].

1.2.3 Properties of CNTs

Carbon nanotubes have gained in interest as nanoscale materials due to their exceptional, outstanding properties such as: extremely high Young's modulus and ultimate strength, high electric and thermal conductivity. Moreover, CNTs provide a remarkable model of a 1D system. More details on the properties of carbon nanotubes are presented below.

1.2.3.1 Mechanical properties

The structural properties of CNTs with strong sigma bonds between the carbon atoms give nanotubes a very high Young's modulus and tensile strength. The strength of the carbon-carbon bonds in-plane, along the cylinder axis, retains the structure exceptionally strong resistance to any failure. CNTs also have very good elasto-mechanical properties. Both experimental and theoretical investigations show extraordinary mechanical properties of individual MWNTs with Young's modulus being over 1 TPa and a tensile strength of 10 - 200 GPa[16-18], which is several hundred times more than that of steel, while they are only one-sixth as heavy. The elastic response of a nanotube to deformation is also remarkable: CNTs can sustain up to 15 % tensile strain before fracture. Nanotubes are shown to be very flexible, with the reversible bending up to angles of 110º for both SWNT and MWNT [19]. Due to the extremely high strength of CNTs, they can bend without breaking. All of these properties open up broad possibilities for the use of CNTs as lightweight, highly elastic, and very strong composite fillers [20].

1.2.3.2 Electrical properties

Carbon nanotubes possess unique electrical properties. The diameter being in the nanometer range gives rise to quantum effects. The differences in the conducting properties are caused by the molecular structure. CNTs can either be conducting or semiconducting, depending on their chirality [21]. They are metallic if the integers of equation (2.1) are: $n=m$ (armchair structure)

and *n-m=3i* (where *i* is an integer). All other structures are predicted to be semiconducting [13]. The geometry of the nanotubes determines band structures and thus the energy band gap. The energy band gap of semiconducting CNTs highly depends on the nanotube diameter and is given by [22]:

$$E_{gap} = \frac{2\gamma_0 \, a_{c-c}}{d} \quad \text{..... (2.2)}$$

Where γ_0 denotes the C-C tight binding overlap energy (2.45 eV), $a_{C\text{-}C}$ the nearest neighbour C-C distance (~1.42 Å), and *d* is the diameter of a nanotube.

Multiwall carbon nanotubes are expected to behave like quantum wires due to the confinement effects on the tube circumferences. The conductance for carbon nanotubes is
given by [10]:

$$G = G_0 M = (2e2/h)M \text{..... (2.3)}$$

where $G_0=(2e2/h)=(12.9kohm)^{-1}$ is the quantum unit of the conductance, *e* is electron charge, *h* is Planck's constant, *M* is an apparent number of conducting channels including electron-electron coupling and intertube coupling effects in addition to intrinsic channels.

In general, MWNTs are quite often found to be one-dimensional conductors with a high electrical conductivity (even $>10^3$ S/cm). The metallic properties of the MWNTs are due to their multiple-shell structure consisting of tubes with various electrical properties, where additional electronic coupling between shells takes place. Moreover, MWNTs are predicted to have ballistic electron transport at room temperature (it refers to conduction where Ohm's law does not apply; the resistance is not dependent on the CNT's length) [24-26]. The electrical current that could be passed through a multiwall nanotube corresponds to a current density in excess of 10^7 A/cm^2 [27].

1.2.3.3 Chemical properties

Functionalization of the carbon nanotubes (chemical or physical modification of the surface of CNTs, e.g. by the attachment of certain molecules or functional groups) is a very important issue in order to overcome their poor solubility in solvents. Functionalized CNTs are very attractive for chemical and biological applications because of their strong sensitivity to chemical or

environmental interactions. This leads to a broad range of applications, e.g. as sensors. Covalent and non-covalent functionalization, doping, decoration with organic as well as inorganic species of the surface of CNTs lead to direct changes of the properties of carbon nanotubes (optical, electrical, and mechanical)[28-32].

1.3 Silica (Sio_2) Nanoparticle

Nanometric metals and inorganic oxides are added to the polymer matrix to improve the mechanical, tribological, and electrical properties of polymer. The macroscopic properties of nanocomposite can be controlled by shape and size and varying the concentration of nanofillers (Caruso, 2001; Nalwa, 2003) [33-34]. The industrial use of silica is widespread from microelectronics to nuclear technology. The excellent electrical and dielectric properties of silica are extensively used in dynamic random access memory and field effect transistors [8-9].

Nanocrystalline silica has been incorporated into a variety of conjugated polymers to obtain better physical properties. Silica is a wide band gap insulator. Impurities and intrinsic defects contribute to ionic conductivity in silica (Roma & Limoge, 2004; Del Frate et al.,1999; Campone et al., 1995) [35-36]. Reasonable conductivity is only found at higher temperature (more than 500 K). Present studies below room temperature rules out the possibility of ionic conduction in silica. The inclusion of dielectric nanocrystal influences the electronic structure of polymers (Musikin et al., 2002) [37]. The insulating behavior of silica and the reduction chain length lead to decrease in conductivity with increase of particle content. Silica nanoparticles are spherical high surface area metal particles. Nanoscale Silicon Particles are typically 5-15 nanometers (nm).

1.4 Nano based composites

The increase in surface to volume ratio in nano particles leads to outstanding properties make them promising filling material or the fabrication of new advanced composite systems for a broad range of applications. Efficient chemical functionalization of nano particles, homogeneous dispersions in solvents and supporting media, and good interconnectivity with matrix still remain very important issues that must be considered in order to achieve heterostructures with enhanced or even new properties. There are numerous methods and approaches for functionalization and further efficient dispersion of the nanoparticles in different media.

1.4.1 Functionalization and dispersion of nano particles

CNTs in all their forms are difficult to disperse and dissolve in any organic and aqueous medium. Due to the strong attractive long-ranged Vander Waals interaction, nanotubes tend to aggregate and form bundles or ropes, usually with highly entangled network structures. This attraction is fundamental for many body particles and well known for colloids dispersed in polymers [34]. When suspended in a polymer, an attractive force between fillers also arises due to the entropic effects [38]. Polymer chains in the region of the colloidal filler suffer an entropic penalty since roughly half of their configurations are precluded. Therefore, there is a depletion of the polymer in this region, resulting in an osmotic pressure forcing the filler particles to come together [39-40]. Homogenous dispersion of CNTs within a supporting medium is crucial for the fabrication of composites with improved properties, well defined and uniform structures. This issue stimulates intensive studies on the exfoliation of carbon nanotubes. Dispersion broadly falls into two main categories: mechanical/physical and chemical methods. The mechanical techniques involve physically separating the tubes from each other. The chemical methods often use surfactant or chemical treatment of the tube surface. However, certain types of aggressive chemical treatment can lead to the key nanotube properties being compromised.

In general, the functionalization of CNTs requires chemical modifications of their surface supported by the mechanical agitation methods such as ultrasonication and shear mixing. Several functionalization strategies have been reported recently. They are mainly based on the covalent ("grafting-to" and "grafting-from"), and noncovalent polymer wrapping [41],stacking interaction, adsorption of surfactants coupling of surfactants and functionalities to CNTs, and is described as follows:

1.4.2 Covalent functionalization: Covalent methods refer to a treatment that involves bond breaking across the surface of the CNTs (e.g. by oxidation) which disrupts the delocalized pie-electron systems and fracture of sigma-bonds and hence leads to incorporation of other species across the CNTs' surface. Introducing defects to the CNT's shell significantly alters the optical, mechanical and electrical properties of the nanotubes and leads to an inferior performance of the composites [42].The advantage is that this kind of modification may improve the efficiency of the bonding between nanotubes and the host material (cross-linking). Therefore, the interfacial

stress transfer between the matrix and CNTs may be enhanced leading to better mechanical performance.

1.4.3 Non-covalent functionalization: This modification of the carbon nanotubes is of great advantage because no disruption of the sp2 graphene structure occurs and the CNT properties are preserved. Its disadvantage concerns weak forces between coupled molecules that may lower the load transfer in the composite.

The chemical modification of the CNTs' surface improves solubility/separation of the nanotubes in a given solvent. A proper functionalization ensures homogenous and stable dispersion throughout the solvent and in the composite host material. Moreover, functionalities on the surface of CNTs may lead to enhanced interactions between filler and matrix due to the presence of the interfacial bonds between components.

1.5 Space charge in solid dielectrics

The behaviour of charge in solid dielectrics has been investigated extensively by many means. Space-charge limited field conduction (SCLC) may result when such charge is trapped [43]. Under a sufficiently strong electric field, the traps may become filled and cause the current to rise by several orders of magnitude to be equivalent to electrical breakdown or ageing. It has been proposed that the presence of persistent space charge can enhance the electrical field locally and is an important factor in determining electrical ageing and breakdown [44]. To obtain a polymeric material with desirable dielectric behaviour, some questions about space charge have to come to mind.

• How does space charge come into being?

• How does space charge behaviour affect the dielectric properties of polymer?

These questions above are discussed in this section.

1.5.1 The origin of space charge in polymer

Generally, space charge may be supplied from the electrode or be generated within the bulk of the polymer. The supply of charge from the electrode involves a transfer of either electrons or holes across the electrode-polymer interface. These processes are strongly dependant on the conditions at the interfaces, which include electrode materials [45], surface defects [43],

impurities [45], and oxidation. The generation of space charge within the bulk of the polymer is usually associated with ionisation of chemical species in the polymer. These may be chemical products introduced during the manufacturing of the material, such as residues of a crosslinking reaction, antioxidant and other impurities [45]. The combination of a spatially inhomogeneous resistivity and current density can be given by

$$\zeta(x) = J\,\varepsilon\,\frac{d\rho(x)}{dx} \quad \text{.....(2.4)}$$

Where ζ is the space charge density, J is the current density, ε is the absolute permittivity, and ρ is the electrical resistivity [46].

1.5.2 The transport of space charge

The accumulation of space charge in a solid will require charge to be transported. It would be possible to ionize a donor site and the electron so removed to proceed through the solid via a series of acceptor states [43]. However the charges of the ionized donor and acceptor states are Coulombically attracted and likely to be strongly coupled [43]. Equally there is the possibility of the hole of the ionized donor proceeding through a series of donor states but the same strong coupling to the electron in an acceptor state will limit this [43]. These situations do not give rise to a net overall space charge in the solid. Production of net space charge (the imbalance between amounts of incoming and outgoing charges) will come about either by electron injection into the solid via acceptor states or electron ejection out of the solid from donor states (hole injection) [43].

1.5.3 Breakdown and space charge

The presence of persistent space charge can distort the electrical field locally and is an important factor in determining electrical ageing and breakdown [43]. Figure 1.6 shows the influence of the heterocharge (figure 1.6a) and homocharge (figure 1.6b) on the interfacial and bulk fields of polymers. If heterocharge is induced at the interfaces near the electrodes, an additional field is formed in this region. This region of heterocharge accumulated has to stand a higher field, figure 2.8a. Contrarily, the local field in the bulk of the matrix is enhanced if homocharge is formed, figure 2.8b.

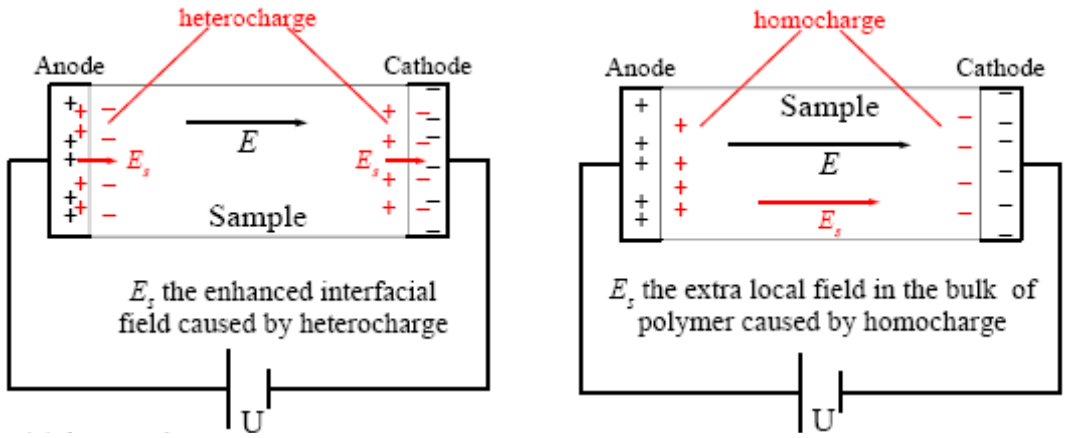

a) heterocharge b) homocharge

Figure 1.6 The detrimental situations to the polymer specimens caused by (a) heterocharge and (b) homocharge

Equation 2.4 indicates that the space charge density is proportional to the current density in the case of a dielectric with a spatially changing resistivity. It is expected that space charge may increase rapidly above a nonlinear threshold in the current density, and, indeed, this has been observed [47]. Space charge is considered one of the major causes of degradation in polymers. It can, of course simple increase the local electrical field in the bulk of insulation or at the electrode-insulation interfaces (as discussed above). However, space charge may involve the storage of electromechanical energy that may increase the degradation reaction rate. Moreover, this causes ionisation, excitation and recombination phenomena that involve considerable energy exchanges which may lead to thermalisation [48] of potential charge carriers.

1.6 Electric conduction mechanisms in polymers

Normally, at the low electrical fields, it is found or assumed that the conduction of electrical current in polymers and insulators is ohmic. However, the polymers electrical properties change when subjected to higher electric fields and temperatures for a long time. The conduction and storage of charge in polymers depends on lots of material parameters such as crystallinity, crosslinking and additives [49]. The electrical conduction mechanisms in composites are complicated. The classical conduction and transport mechanisms found in conductors and semiconductors are not found in polymers. This is due to the difference of morphology and chemistry of the polymer. Consequently different mechanisms operate. Charge injection from electrodes into polymer, traps and volumetric conduction, tunneling and hopping conduction

were found to play an important role in conduction and charge transport in polymers. Electric conduction may therefore depend on material preparations and their thermal history and it becomes very difficult to determine the conduction mechanism. In general, electric conduction may occur through the movement of either electrons (holes) or ions. The conductivity σ varies exponentially with temperature and can be described as

$$\sigma = \sigma_0 \exp\left(\frac{\varphi}{KT}\right) = \Sigma q_i n_i \mu_i \quad \text{.....(2.5)}$$

where σ_0 is a material constant, φ is the activation energy, k is the Boltzmann constant, is the temperature, q_i , n_i and μ_i is the charge, the density and the mobility of the spices, respectively. The steady state conduction current in composites is controlled by either electrode or bulk processes. Usually, more than one mechanism may operate at the same time, but only one is dominating.

1.6.1 Electronic processes

Under a high external field, many electrons may be injected into polymers from the cathode. However, the condition of the electrode-insulator interface is very complicated [44]. Electrical, chemical and physical defects are likely to exist at the interface. Such defects include protrusions, imperfect contacts, dangling bonds, and local polarization, contaminants, and traps. Electrons are injected from electrodes into the bulk of material. Electrons need to overcome a potential barrier to cross from electrode into insulator. Crossing the barrier depends on applied electric field and the interface defects.

1.7 Literature Review

Poly(vinylidene fluoride) (PVDF) is one of the semi crystalline polymers with at least four crystalline forms referred to as α,β and γ phase, among which the β-phase has gained substantial importance due to its advantageous pyro and piezo-electric properties [49- 50]. It requires a better method to induce the formation of β-phase crystal in order to improve the electrical properties of PVDF. β-phase is not usually obtained by crystallization from the melt, but it is normally obtained by various methods including tensile deformation and uniaxial compressional deformation of a phase, blending with small contents of poly(methyl methacrylate) (PMMA) or poly(omethoxyaniline) (POMA), quenching and then annealing process [51-52], applying a

strong electric field and crystallizing from solution at appropriate conditions [53-55]. In all these methods which used to prepare β-phase of PVDF, the one grown from a single solvent is widely used because of its facility and controllability. However, few literatures are concentrated on the solvent induced β-phase formation in the mixed solvent.

Ma.et al. [54] concludes that DMF content in the mixed solvent has a definite effect on the crystalline phase of PVDF and the resulting morphology of the films. As PVDF crystallized from a THF/DMF solution at 50^{o}C, the resulting crystalline phase depended on the THF/DMF mass ratio. In particular, the content of the β-phase in the cast film can notably be influenced by the incorporation of DMF in the mixed solvents. The best solubility and the stronger interaction between the PVDF chains and DMF molecules can dramatically favor the β crystal formation. The mixed solvent at a 5/5 ratio resulted in the clear spherulitic structure with a diameter of about 3 μm on the surface of the film.

Nanoparticles in polymer have attracted tremendous attention due to their extraordinary mechanical, electronic, and optical properties. Numerous potential applications (such as sensors,emission tips, electronic device, etc.) have been proposed. Poly(vinylidene fluoride) (PVDF) and its copolymers have attracted more attentions for their broad applications in electromechanical systems. Lots of methods were employed to enhance the dielectric constant of the PVDF matrix. By doping ceramic, semiconductor, metal, metal oxide and carbon nanotubes (CNTs) component, the dielectric constants of the PVDF composites were enhanced .However, the polymer, which was filled with much ceramic, semiconductor, metal, will lose its flexibility. Until now, the dielectric constants, which were achieved in all polymer composites above, were only several hundreds [55].

The excellent electrical and dielectric properties of silica are extensively used in polymers. Encapsulated nanosilica are also synthesized in poly(methylmethactylate) with distinct morphology (Chen et al., 2004)[56]. The nucleation density and the crystallization rates are significantly increased by silica nanofillers in poly(tetramethyleneterephthalamide). Conducting polymers such as polyaniline (PANI) and polypyrrole (PPY) are used as host matrix for the dispersion of inorganic nanoparticles. The most general method to obtain conducting polymer nanocomposite with oxide nanoparticles is direct polymerization method.

In order to enhance the physical properties of CNTs, the chemical functionalization has been introduced in recent years. The chemical functionalization consists of the covalent functionalization and noncovalent functionalization. The noncovalent functionalization has been investigated intensively, for instance, the surfactant has been adopted to improve the dispersion of CNTs in the polymer composites. Besides, the polymer wrapped CNTs by in situ polymerization and the covalent functionalizations, for instance, the carboxylic, amine, ester functionalizations, were also investigated widely before. (Dang et al)[57] MWNTs were modified with 3,4,5-trifluorobromobenzene (TFBB) in order to improve their dispersal in PVDF. After treatment, there was a strong interaction between the trifluorophenyl (TFP)-functionalized MWNTs and PVDF because of the number of fluoride groups existing on the surface of the TFP-MWNTs. Furthermore, functionalization of the MWNTs with TFBB created a novel MWNT/PVDF EAPC, which displayed a giant dielectric permittivity (ε ~8000) over a critical content of TFP-MWNTs, while retaining the flexibility of the polymer matrix used [13].

Recently, (Harmon *et al*.)[58] produced conductive and transparent CNT-polymer composites through a combination of dispersion through sonication, in- situ polymerization, dissolution and film casting, in which, the nanotubes were mixed with deinhibited methyl methacrylate (MMA) and dispersed by sonication.

In 2001, Dupire *et al*. patented [59] a method for the production of reinforced polymer, in which both the polymer chains and carbon nanotubes were oriented and dispersed by stretching the nanotube-polymer mixture in a molten state and in a solid state using a high shear mixer. However, the resulting nanocomposites exhibited limited transparency in the visible range.

Niu *et al*. [60] revealed a method for the preparation of mechanically strong yet electrically conductive polyvinylidene fluoride, (PVDF)-CNT composite by two different methods. In solution method, PVDF was first dissolved in a solvent such as acetone, CNTs were then added into the solution and sonicated. The composite was then precipitated with a precipitating component such as water, filtered and dried. In melt compounding method, PVDF was mixed with CNTs in a mixer at high temperatures to melt and compound PVDF into CNTs to form the composite. They found that the composite prepared by the solution method were better electrical conductors than that by the melt compounding method. They claimed that this composite had a higher level of conductivity than other known polymer composites.

1.8 Aim of work and objective

In polymers family, Poly(vinylidene fluoride) (PVDF) is material of extensive research due to its piezoelectric, pyroelectric and ferroelectric behaviour and become effective and durable in different environments for various technological applications. The literature review gives an idea that the electrical properties of polymer can be enhanced by mean of adding nanoparticles (Carbon nanotube, silica naoparticles) where the concentration of carbon nanotube can be varied from 0.5 to 20% by weight of polymer composite.The main objective of the study is to produce and investigate nano based composites for next generation having high-strength, lightweight, and conductive plastics using nanoparticles. However, the effective utilization of nanoparticles in composite applications strongly depends on the ability to disperse them homogeneously throughout the matrix.

In this work, Muti-wall carbon nanotubes (MWNT) and Silica nanoparticle with different weight fractions are dispersed in poly(vinylidene fluoride) matrix to make composite. The major challenge is to homogenous dispersion of the MWNT in the matrix because due to vander walls forces between the nanotubes, they tend to agglomerate. The surface of CNTs has to be modified in order to overcome their poor solubility and reactivity. A uniform distribution of nano particle within a polymer matrix and strong adhesion between structural components are necessary conditions for the effective improvement of the properties of the composites. In this study we focused on the evolution of the structural and physical properties of nano dispersed composite systems.

The main objectives are:

1) Synthesis of β-phase in poly(vinylidene fluoride) PVDF polymer
2) Functionalization of nano materials.
3) Synthesis of nano based polymer composite.
4) Characterization of nano composite by using various techniques.

Chapter-2
Methodology

2.1 Materials

The materials used in this study were poly(vinylidene)fluoride PVDF (pellet) typical M_w =530.000 (Aldrich), Multiwall carbon nanotubes MWNTs with "hollow" and "bamboo" morphologies having diameter in the range of 110-170 nm, lengths between 5-9 micron, and purities of 98% (Aldrich), Silicon dioxide SiO_2 nanopowder with particles size 5-15 nm (BET) 99.5% metal basis (Aldrich). The solvents used during synthesis were tetrahydrofuran (THF), C_4H_8O (Mw=72.11, stablized) (s.d.fine-chem Ltd) and N ,N-Dimethylformamide DMF, C_3H_7NO (MW=73.09) (s.d.fine-chem Ltd). All the materials used as received without any further purification except CNT's and nanoparticles.

2.2 Synthesis of β-phase Poly(vinylidene fluoride) (PVDF)

The glass wares (three necks round bottom flask, measuring cylinder and beaker) were first cleaned and rinse with distilled water and dried in vacuum oven. All the materials and solvents were weighted with help of electronic weighing balance and mixed in cleaned round bottom flask.

Figure 2.1 Experimental set up for the sample preparation.

A 100 ml three neck flask charged with 10g poly(vinylidene fluoride) (Typical M_w = 530.000) (Aldrich) dissolved in THF/DMF mixture with different mass ratio (m/m composition of THF/DMF = 9:1, 8:2, 7:3 and 5:5). All the reactions were refluxed at 60^{o}C with gentle stirring for 3h on hot plate shown in figure 2.1.

After stirring for 3h, reaction mixture allowed to cool to room temperature. The transparent solution was cast on glass substrates by spin coating and rest of the solution pour into beaker to prepare thin film and bulk film. The residue of DMF and THF was allowed to evaporate in an air oven for about one week at room temperature. Free-standing thin films (thickness ~ 4-6 μm) on glass substrate and bulk film (thickness ~ 1-1.5 mm) were formed in the end when the solvent was completely evaporated.

2.2.1.1 Chemical composition

Table1: Sample 1 THF: DMF (9:1)

Sr.No.	Chemical name	Chemical formula	Material taken
1	Poly(vinylidene fluoride) (PVDF)	-(CH_2 -CF_2)-	1g
2	Tetrahydrofuran (THF)	C_4H_8O	9ml
3	N ,N-Dimethylformamide (DMF)	C_3H_7NO	1ml

Table2: Sample 2 THF: DMF (8:2)

Sr.No.	Chemical name	Chemical formula	Material taken
1	Poly(vinylidene fluoride) (PVDF)	-(CH_2 -CF_2)-	1g
2	Tetrahydrofuran (THF)	C_4H_8O	8ml
3	N ,N-Dimethylformamide (DMF)	C_3H_7NO	2ml

Table3: Sample 3 THF: DMF (7:3)

Sr.No.	Chemical name	Chemical formula	Material taken
1	Poly(vinylidene fluoride) (PVDF)	$-(CH_2-CF_2)-$	1g
2	Tetrahydrofuran (THF)	C_4H_8O	7ml
3	N ,N-Dimethylformamide (DMF)	C_3H_7NO	3ml

Table4: Sample 4 THF: DMF (5:5)

Sr.No.	Chemical name	Chemical formula	Material taken
1	Poly(vinylidene fluoride) (PVDF)	$-(CH_2-CF_2)-$	1g
2	Tetrahydrofuran (THF)	C_4H_8O	5ml
3	N ,N-Dimethylformamide (DMF)	C_3H_7NO	5ml

2.2.1.2 Spin coating

Spin coating is the preferred method for deposition of thin and uniform films on flat substrates. In the typical procedure the appropriate amount of polymer solution is poured in the center of the substrate.

Figure 2.2 Spin coating unit

The substrate is then rotated at high speed in order to spread the fluid by centrifugal force. Rotation is continued for some time, with fluid being spun off the edges of the substrate, until the desired film thickness is achieved. The solvent is usually volatile, providing for its simultaneous evaporation with the passage of time.

2.2.1.3 Cell preparation for dielectric studies

Dielectric measurement of thin film samples were carried out by depositing thin film on ITO coated glass substrate in spin coating unit and sandwiches by another ITO coated glass plate followed by sealing and electrical connection. To make cell (capacitor) schematic of thin film assembly shown in figure2.3 and figure2.4 shows prepared samples for dielectric studies of thin film.

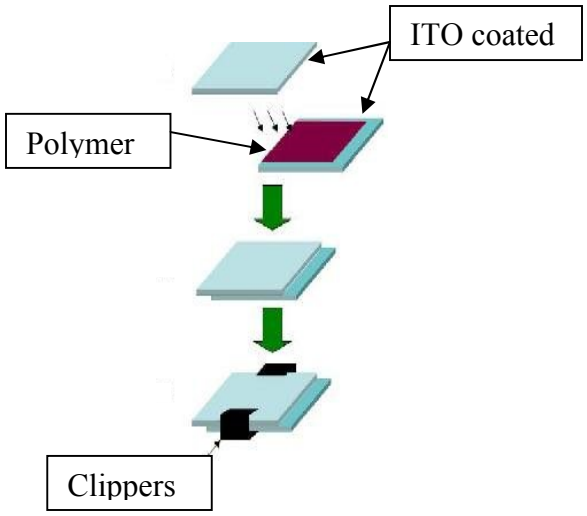

Figure 2.3 Schematic of thin film assembly

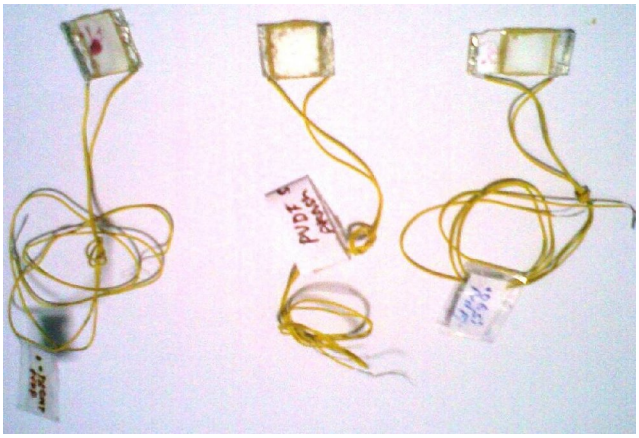

Figure 2.4 Prepared cells for dielectric studies

2.3 Functionalization of MWNTs and SiO_2 nanoparticles

Multiwall carbon nanotubes and Silicon dioxide SiO_2 nanoparticles were functionlized in order to achieve a good level of exfoliation of the bundles and agglomerations of CNTs and SiO_2 nanoparticles and to make them reactive for better chemical linkage. Since chemical modification of CNTs and SiO_2 nanoparticles is crucial for obtaining uniform dispersions and chemical stability of nanotubes in organic or aqueous solvents, the covalent functionalization of the surface of MWNTs and SiO_2 nanoparticles were introduced.

2.3.1 Oxidation of MWNTs with acids

The MWNTs (37.88 mg) were chemically functionalized by ultrasonification in a mixture of 3M of concentrated sulphuric acid and 1M of concentrated nitric acid (3:1) for 2h at 50°C temperature, finally 1M HCL was added and mixture sonicated for ½ h at 50°C. After the completion of reaction the mixture was diluted with deionised water and then vacuum-filtered through a polycarbonate membrane. After filtration the acid-oxidized MWNTs were washed with deionised water in order to obtain pH value around 7 and then dried at 60°C for 12h. These acid treatments may shorten the length of the MWNT and introduce carboxylic acid groups.

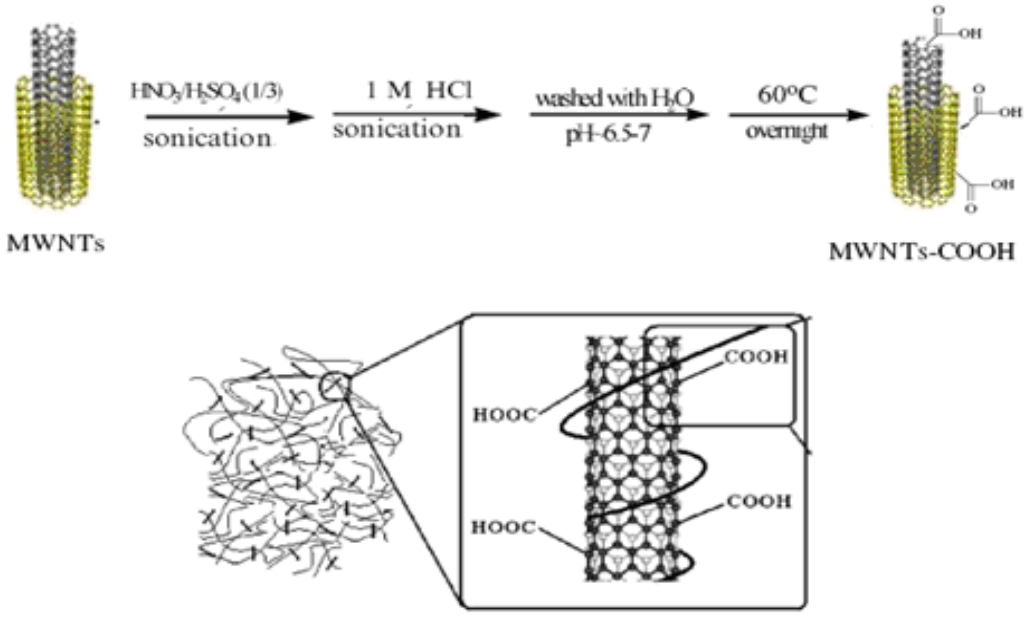

Figure 2.5 Schematic of covalent functionalization of the oxidized CNT.

Oxidation disrupts the π bonding symmetry of the sp^2 hybridize carbon atoms and therefore leads to numerous side defects along the entire length of CNTs. Oxidized CNTs (carboxylic groups are

dominant, therefore the CNT-COOH abbreviation is used to refer to oxidized nanotubes) remain stable in aqueous solvent for months The schematic of covalent functionalization of the oxidized CNT as shown in figure2.5. Further the functionalized CNTs were characterised by FTIR to confirm the functionlization.

2.3.1.1 Chemical composition for functionlization of MWCNTs

Table 5:

Sr.No.	Chemical name	Chemical formula	Material taken
1	Multiwall carbonnanotube	-(C=C)-	37.88mg
2	Sulphuric acid	H_2SO_4	15ml
3	Nitrric acid	HNO_3	5ml
4	Hydrochloric acid	HCl	1ml
5	Distilled water	H_2O	10ml

2.3.2Oxidation of SiO_2 nanoparticles with acids

The same procedure was employed in order to functionlized the silica nanoparticles as CNTs. After the completion of reaction mixture was diluted with deionised water and then centrifuged the solution for 15 min. After filtration the acid-oxidized SiO_2 were washed with deionised water in order to obtain pH value around 7 and then dried in oven at 40^oC temperature for 4h. Schematic of covalent functionalization of the oxidized silica nanoparticles shown in fig.2.6. Further the functionalized silica nanoparticles were characterised by FTIR to confirm the functionlization.

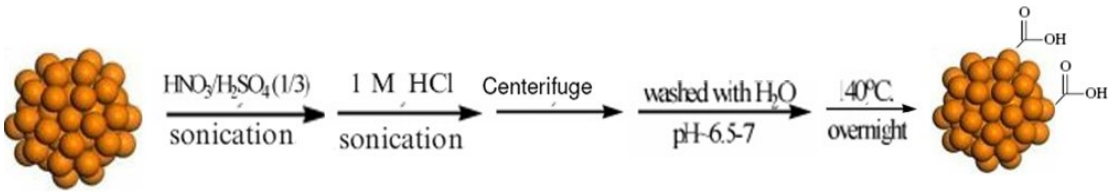

Figure2.6 Schematic of covalent functionalization of the oxidized silica nanoparticles.

2.3.2.1Chemical composition

Table 6:

Sr.No.	Chemical name	Chemical formula	Material taken
1	Silica nano particle	SiO_2	100mg
2	Sulphuric acid	H_2SO_4	15ml
3	Nitrric acid	HNO_3	5ml
4	Hydrochloric acid	HCl	1ml
5	Distilled water	H_2O	10ml

2.4 Polymer-Composite preparation

2.4.1 Solution processing of MWNT-PVDF composite

In order to prepare composite system the first step was same as the synthesis of PVDF samples. In Second step, an appropriate amount of functionlized MWNT was added to mixture of (PVDF) poly(vinylidene)fluoride, an organic solvent N,Ndimethylformamide (DMF) and tetrahydrofuran (THF). The final mixture was gently refluxed at 60^{o}C for 3h after stirrering, the solution was sonicated for 2h. After the addition of CNT the colour of solution turned black which confirms dispersion of CNTs in PVDF matrix. The MWNT-PVDF samples were prepared with different concentrations of CNTs in PVDF. This final mixture is further treated for making of thin film and bulk films by using various techniques i.e. Spin Coating and Solution Cast Method. The residue of DMF and THF was allowed to evaporate in an air oven for about week at room temperature. Free-standing thin films (thickness~4-6 μm) on glass substrate and bulk film (thickness~1-1.5 mm) were formed at the end when the solvent completely evaporated.

2.4.1.1 Chemical composition

Table7:Sample1, PVDF-MWCNT Composite (0.02wt%, 0.06wt%, 0.08wt%, 0.1wt %)

Sr.No.	Chemical name	Chemical formula	Material taken
1	Poly(vinylidene fluoride) (PVDF)	$-(CH_2-CF_2)-$	1g
2	Multiwall carbonnanotube	-(C=C)-	0.02,0.06,0.08,0.1mg
2	Tetrahydrofuran (THF)	C_4H_8O	5ml
3	N ,N-Dimethylformamide (DMF)	C_3H_7NO	5ml

2.4.2 Solution processing SiO_2 –PVDF of composite

An appropriate amount of functionalized SiO_2 nanoparticles was added to mixture of PVDF poly(vinylidene)fluoride , an organic solvent (DMF) N,Ndimethylformamide and (THF) tetrahydrofuran. The final mixture was then thoroughly mixed by magnetic stirrer at 60^oC for 3h. After stirrering, the solution was sonicated for 2h. The SiO_2 nanoparticles -PVDF samples were prepared with different wt% of PVDF. This final mixture is further treated for making of thin film and bulk films by using various techniques i.e. spin coating and solution cast method. The residue of DMF and THF was allowed to evaporate in an air oven for about one week at room temperature. Free-standing thin films (thickness ~ 4-6 μm) on glass substrate and bulk film (thickness ~ 1-1.5 mm) were formed in the end when the solvent completely evaporated.

2.4.2.1Chemical composition

Table 8: PVDF-Silica Composite for 0.02 wt%, 0.06wt%, 0.08wt%, 0.1wt%

Sr.No.	Chemical name	Chemical formula	Material used
1	Poly(vinylidene fluoride)	$-(CH_2-CF_2)-$	1g
2	Silica nanoparticle	SiO_2	0.02,0.06,0.08,0.1mg
2	Tetrahydrofuran	C_4H_8O	5ml
3	N ,N-Dimethylformamide	C_3H_7NO	5ml

2.5 Characterization Techniques

The morphological and dielectric measurments of the nanocomposites characterized by using various experimental techniques including Olympus optical polarizing microscope (Model BX51P), Fourier transformation IR Spectroscopy (FTIR, Perkin-Elmer BX-II), X-ray diffraction (XRD, Rigaku), Scanning Electron Microscope (SEM), LCR meter FLUKE PM 6306 (frequency range 50Hz to 1MHz) and LCR meter Agilent 4284A (frequency range 20Hz to 1MHz).

2.5.1 Optical polarizing microscopy

The optical studies observed in pure PVDF, MWCNT and SiO_2 dispersed PVDF systems investigated using an Olympus optical polarizing microscope (Model BX51P) at a magnification of 10X under crossed polarizer using long working distance objective lens. A block diagram of our experimental set-up for the investigation of optical textures, dielectric studies and other parameters of liquid crystal is shown in figure 2.7.

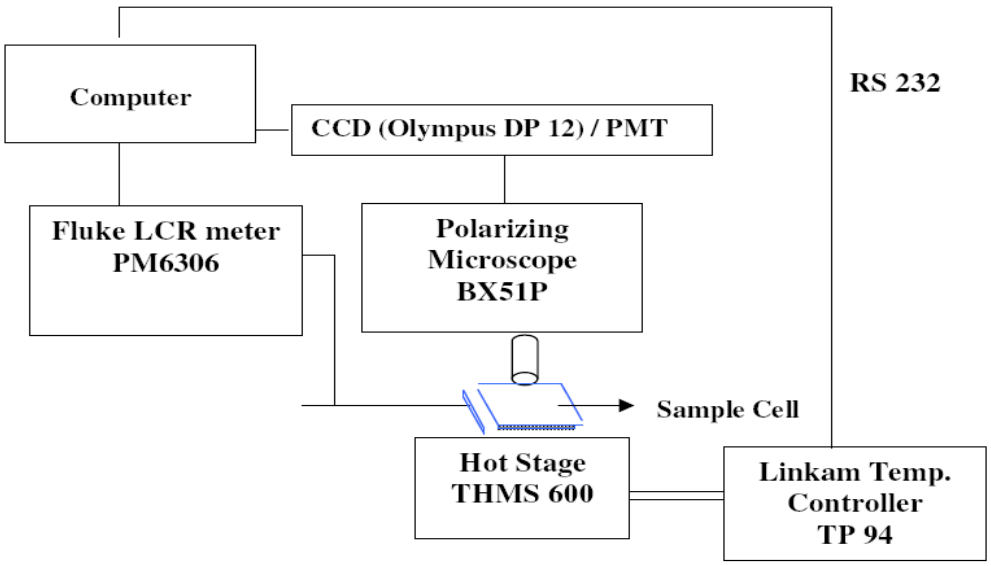

Figure 2.7 Block diagram of the experimental set-up to study the morphological and dielectric studies of PVDF composite systems.

In dielectric studies, we used Linkam temperature programmer TP94 and hot stage THMS 600. The TP94 is specifically designed for precise temperature control of the Linkam heating/freezing

stages. The stage sensor is digitally linearized to give accurate temperature readout, the controls and their functions have been carefully chosen for simple and easy operation. The temperature range is –196 ^{0}C to 600 ^{0}C. Heating or cooling rates can be changed almost instantly using the three rate keys. The heat ranges are from 0.1 to 0.9^{0}C/min at 0.1 degree intervals from 1.0 to 9.0 ^{0}C/min at 1.0 degree intervals.

2.5.2 Fourier transformation IR Spectroscopy

FT-IR stands for Fourier Transform Infrared, the preferred method of infrared spectroscopy. The prepared samples were characterised by via HATR, FTIR spectroscopy. The experimental set up is shown in figure2.8. In infrared spectroscopy, IR radiation is passed through a sample. Some of the infrared radiation is absorbed by the sample and some of it is passed through (transmitted). The resulting spectrum represents the molecular absorption and transmission, gives information of type of bonding in the sample. This makes infrared spectroscopy useful for several types of analysis.

Figure 2.8 Fourier transform infrared (FTIR) spectrometry

So, what information can FT-IR provide?

• It can identify unknown materials

• It can determine the quality or consistency of a sample

• It can determine the amount of components in a mixture.

The original infrared instruments were of the dispersive type. These instruments separated the individual frequencies of energy emitted from the infrared source. This was accomplished by the use of a prism or grating. A grating is a more modern dispersive element which better separates

the frequencies of infrared energy. The detector measures the amount of energy at each frequency which has passed through the sample. This results in a spectrum which is a plot of intensity vs frequency. Fourier Transform Infrared (FT-IR) spectrometry was developed in order to overcome the limitations encountered with dispersive instruments. The main difficulty was the slow scanning process. A method for measuring all of the infrared frequencies simultaneously, rather than individually, was needed. A solution was developed which employed a very simple optical device called an interferometer. The interferometer produces a unique type of signal which has all of the infrared frequencies "encoded" into it. The signal can be measured very quickly, usually on the order of one second. Thus the time element per sample is reduced to a matter of a few seconds rather than several minutes.

2.5.3 X-ray diffraction

X-ray diffraction is non-destructive analytical techniques which reveal information about the crystallographic structure, chemical composition, and physical properties of materials and thin films. Characterization of crystalline phase in thin films was done by XRD (Rigaku) as shown in figure 2.9.

Figure 2.9 X-ray diffractrometer

This technique is based on observing the scattered intensity of an X-ray beam hitting a sample as a function of incident and scattered angle, polarization, and wavelength or energy. X-ray diffraction is an experimental technique that exploits the fact that X-rays are diffracted by crystals. X-rays have the proper wavelength (in the Angstrom range, ~10^{-8} cm) to be scattered by

the electron cloud of an atom of comparable size. Based on the diffraction pattern obtained from X-ray scattering off the periodic assembly of molecules or atoms in the crystal, the electron density can be reconstructed. Additional phase information must be extracted either from the diffraction data.

2.5.3.1Wide angle X-ray diffraction

Wide angle X-ray diffraction (WAXD) is an X-ray diffraction technique that is often used to determine the crystalline structure of materials. This technique specifically refers to the analysis of Bragg Peaks scattered to wide angles, which (by Bragg's law) implies that they are caused by sub-nanometer sized structures. Wide angle x-ray scattering is the same technique as Small-Angle X-ray Scattering (SAXS) only the distance from sample to the detector is shorter and thus diffraction maxima at larger angles are observed .A diffraction technique for polycrystalline films where only crystallites diffract which are parallel to the substrate surface. The diffraction pattern generated allows to determine the chemical composition or phase composition of the film, the texture of the film (preferred alignment of crystallites), the crystallite size and presence of film stress. According to this method the sample is scanned in a wide angle X-ray goniometer, and the scattering intensity is plotted as a function of the 2θ angle. X ray diffraction is a non destructive method of characterization of solid materials. In fact solids with the same chemical composition but different phases can be identified by their d spacing.

2.5.4 Dielectric measurements

The dielectric measurements were carried out using a programmable automatic RCL meter (FLUKE PM 6306) in the frequency range 50Hz to 1MHz (fig.2.10a) for thin films and Precision RCL meter (Agilent 4284 A) in the frequency range 20Hz to 1MHz (fig.2.10b) for bulk films. The frequency dependence of the real and imaginary parts have been studied in detailed at different temperatures. The dielectric properties of the PVDF composites were also taken at off voltages. Measurement in the high frequency range has been limited to 1 MHz because of the dominating effect of finite resistance of ITO coating on glass plates and lead inductance.

(a)

(b)

Figure 2.10 LCR Meter, (a) FLUKE PM6306 (b) AGILENT 4284 A set up

In the case of polymeric medium, dielectric spectroscopy is a useful technique to understand the dielectric behaviour. The complex dielectric properties, the relative permittivity (ε') and the loss factor (ε") were determined as a function of frequency and temperature. The dielectric constant ε' is calculated by formula given below:

$$\varepsilon' = \frac{Cd}{A\varepsilon_0} \quad \text{.....2.6}$$

Where C is the capacitance, d is the thickness of the sample, A is the area of the parallel electrodes and ε_0 is the dielectric permittivity of vacuum (ε_0 = 8.85 x 10-12 F/m). The dielectric constant of the material depends on the material's polarization, the higher the polarizability of the molecules, the higher the dielectric constant.

3.1 Morphological behaviour of pure and nano dispersed PVDF system

3.1.1 MWCNTs dispersed PVDF thin film and bulk samples

Optical micrographs of thin film and bulk samples of pure, CNT dispersed PVDF at different concentrations are shown in figure3.1 and 3.2. respectively. It was observed that CNTs were well dispersed in PVDF matrix as evident from figure3.1 (a to d) respectively. We found that in bulk samples the morphology was disrupt and some voids were present in the samples. Figure3.3 and 3.4. shows optical micrographs of thin film and bulk samples of pure and SiO_2 dispersed PVDF at different concentrations. It was clearly observed from above micrographs that the sample prepared for various concentrations of MWCNTs and SiO_2 were uniformly dispersed and have less porosity. The black spots on micrographs could be due to the voids in thin film and bulk samples.

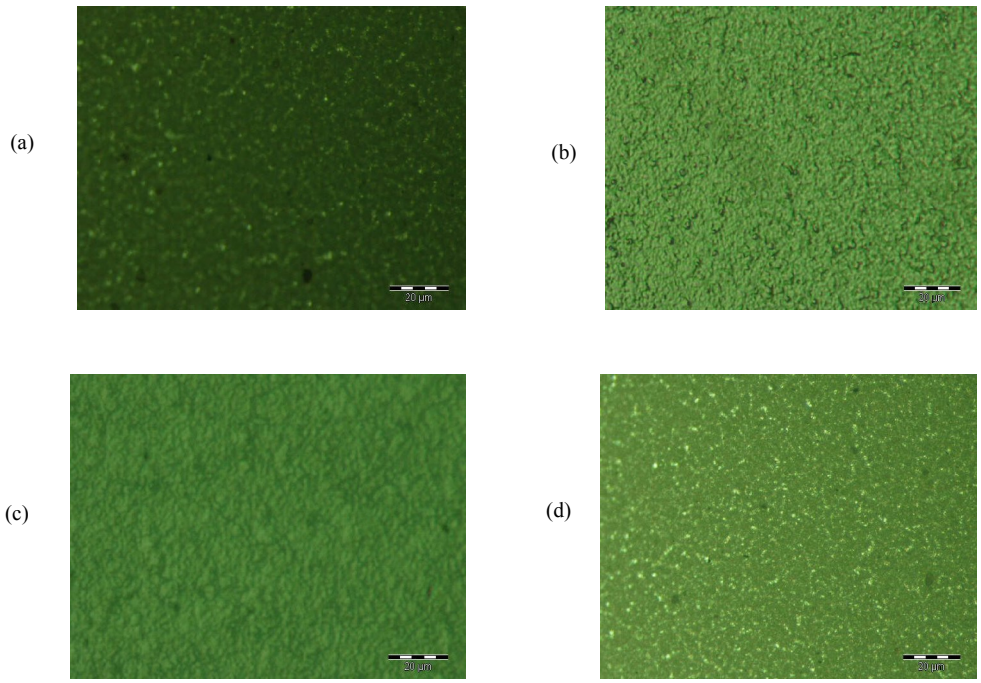

Figure 3.1 Morphology of PVDF-MWCNT composites thin films; a) Pure; b) 0.02% MWCNT; c) 0.06% MWCNT; d) 0.08% MWCNT

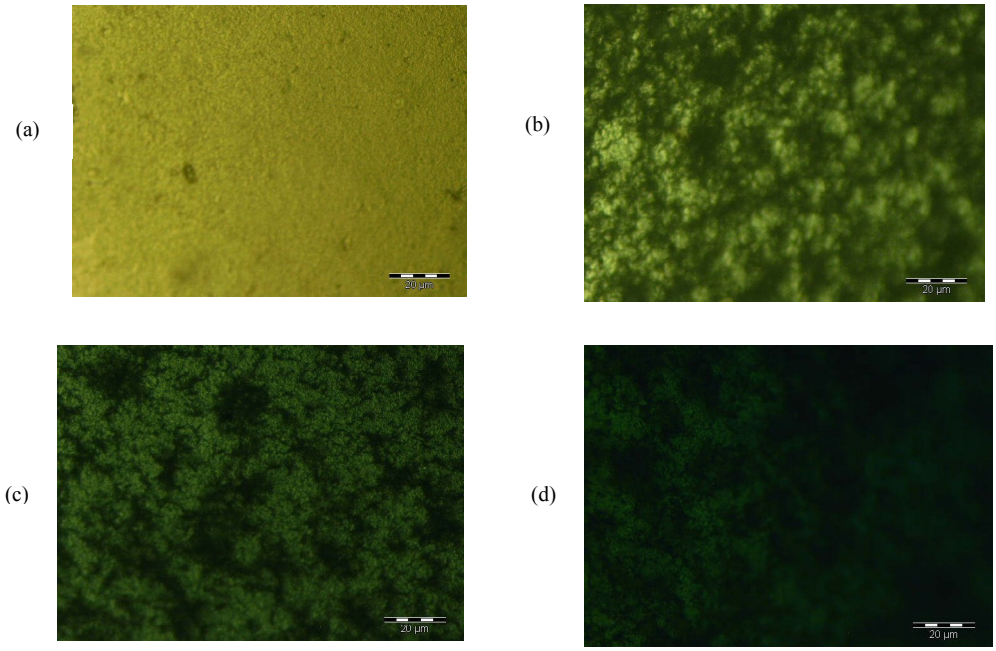

Figure 3.2 Morphology of PVDF-MWCNT composites bulk samples; a) Pure; b) 0.02% MWCNT; c) 0.06% MWCNT; d) 0.08% MWCNT

3.1.2 SiO_2 dispersed PVDF thin film and bulk samples

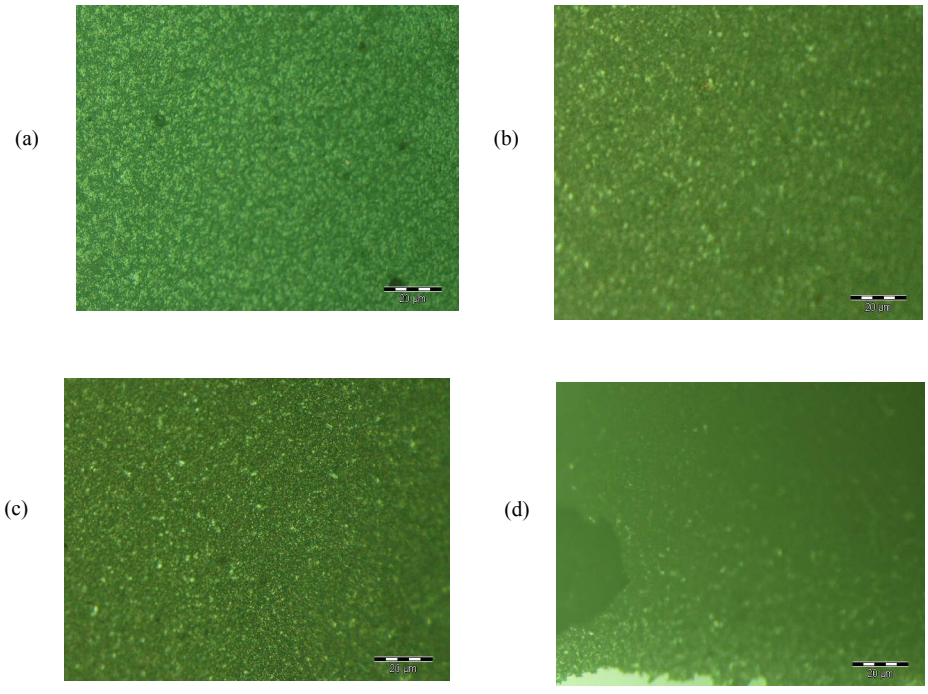

Figure 3.3 Morphology of PVDF-SiO_2 composites thin films; a) 0.02% SiO_2; b) 0.06% SiO_2; c) 0.08% SiO_2; c) 0.08% SiO_2

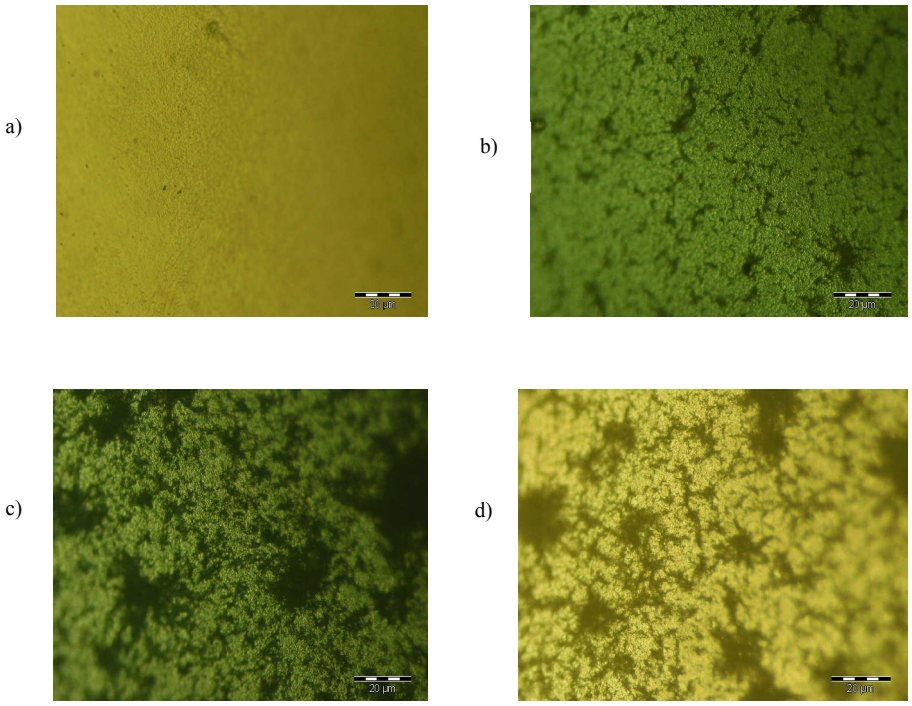

Figure 3.4 Morphology of PVDF-SiO_2 composites bulk samples; a) Pure; b) 0.02% SiO_2 ; c) 0.06% SiO_2; d) 0.08% SiO_2

3.2 Chemical analysis

FTIR spectra (range from 4000 to 400 cm^{-1}) of the thin films for mixed solvents (THF/DMF) in the ratio 5:5, 7:3, 8:2 and 9:1 is shown in figure 3.5.

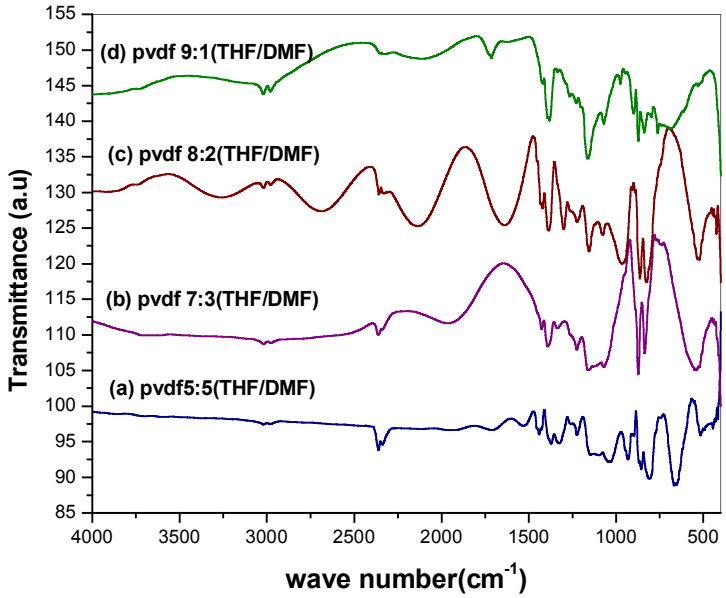

Figure 3.5 FTIR spectra of PVDF films cast by spin coating in the mass ratio of THF/DMF: (a) 5:5; b) 7:3; c) 8:2; d) 9:1 respectively.

In the thin film containing 5:5 (THF/DMF) wt/wt ratio, we observed transmission peaks at 417.91, 761.36, 855.87 and 974.92 cm^{-1} corresponds to α-phase, while the peaks at 515.98, 445.72 and 842.86 cm^{-1} are indicative of β-phase. The peaks observed at 1030.32, 1076.71, 1070.09 cm^{-1} corresponds to fluoro alkane. Some additional peaks at 3018 cm^{-1} and 3019.77cm^{-1} refers to the antisymmetric stretching of CH_2 while the band at 2976.02 cm^{-1} observed corresponds to vinyl group. we conclude that as the concentration of DMF increased the α-phase decreased and disappeared at higher concentration of DMF as evident from the IR spectra of 8:2, 7:3 and 5:5 composition respectively.The solubility of the PVDF was improved by an increase of DMF content in the mixture of solvents because of the reinforced disruption of the intermolecular polymer bonds (via interaction of the C = O dipole with the CH_2CF_2 dipole or by limited hydrogen bonding). PVDF is wholly responsible for the vibration occur in the region of 400 to 1330 cm^{-1}. Vibration modes observed in the region of 1000 to 1330 cm^{-1} influence the dipole moment, which gives rise to the alignment of dipoles and responsible for the polarization in β-phase.

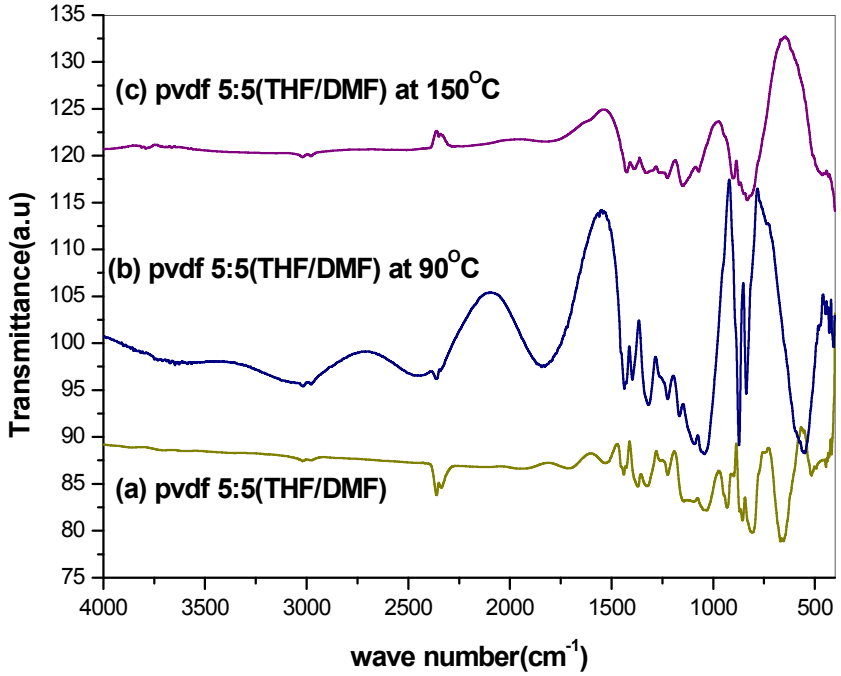

Figure 3.6 FTIR spectra of PVDF films cast with mass ratio of 5:5 (THF/DMF): a) without heated; b) at 90°C; c) at 155°C

Figure 3.6 shows the FTIR spectra of thin film annealed at 90°C and 155°C. After annealing at 90°C for 5h, we observed that the β–phase was dominant and α–phase got suppressed. However

when film was annealed at higher temperature 155^{o}C (5h), the α-phase became prominent as shown in figure3.6(c)**.**

3.3 Structural analysis of β-phase in Poly(vinylidene fluoride) (PVDF)

Wide angle X-ray diffraction (WAXD) was used to identify the crystalline phase of PVDF sample. Figure 3.7 shows X-ray pattern of the film heated at 90^{o}C (THF/DMF = 5/5), the peaks present at 2θ = 18.58^{o} and 19.94^{o} respectively refer to the diffractions in planes (020) and (110) respectively, which shows existence of α-phase in PVDF. In addition, a peak at 2θ = 20.2^{o} refers to the sum of the diffractions in plane (110) and (200), characteristic of the β-phase. We also made an attempt to study the effect of annealing at higher temperature (155^{o}C)**.** The XRD pattern recorded for PVDF thin film at 155^{o}C is shown in figure 3.7(b). The peaks observed at 2θ = 18.42^{o}, 19.28^{o} corresponds to planes (020) and (110) respectively are indicative of α-phase, only one characteristic peak with very low intensity observed at 2θ = 20.6^{o} is indicative of β-phase. It clearly reflects that the temperature gradient plays important role in the phase change and crystallinity in PVDF.

The crystallinity in the PVDF sample was enhanced, after annealing at 90^{0}C, above α-relaxation temperature, the conversion rate from α to β phase occurs due to motion of conformers without considerable deformation in the crystals and increase in β–phase has been observed. This may be due to the fact that at annealing temperature (90^{0}C), the viscosity of the material decreases but still high enough to prevent the orientation of crystals, but the chain mobility increase enough to recognize the structure of conformers, which allow the active chain motion and chain reorientation in crystalline region through the trans-guche conformational exchange of β–phase. At this temperature crystallization rate of β–phase is higher as compare to other phases. In the β–phase of PVDF the long trans zigzag segmenta are connected to each other with skew bond or equivalent gauche-trans sequences.

At higher annealing temperature (155^{o}C), the β–phase of PVDF decreases, due to deformation in crystalline region and with reorientation of chains, more stable α-phase could have reappeared in PVDF film.

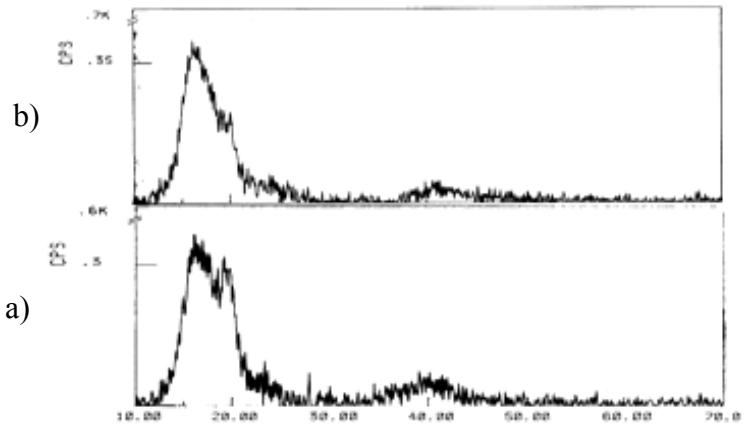

Figure 3.7 X-ray pattern of annealed PVDF films prepared in (THF/DMF = 5/5); (a) at 90°C; (b) at 155°C.

3.4 Synthesis of PVDF-MWCNT composite

3.4.1 FTIR spectra of functionalized MWCNT by Carboxylic group

FTIR spectrum of pure and functionalised MWCNTs showed (fig 3.8a) broad transmission peak at 3305 cm^{-1} due to OH group of carboxylic acid, in the spectrum, the peak of the carbonyl groups of the carboxylic anions observed at 1538cm^{-1} confirms functionalization of the MWCNTs and acidification by hydrochloric acid causes stretching vibration in carbonyl groups at 1710 cm^{-1}. The signal at 3734 cm^{-1} is attributed to the unassociated carboxyl groups and peak at 1638cm^{-1} (fig.3.8b) corresponds to C=C (both sp^2) of CNT.

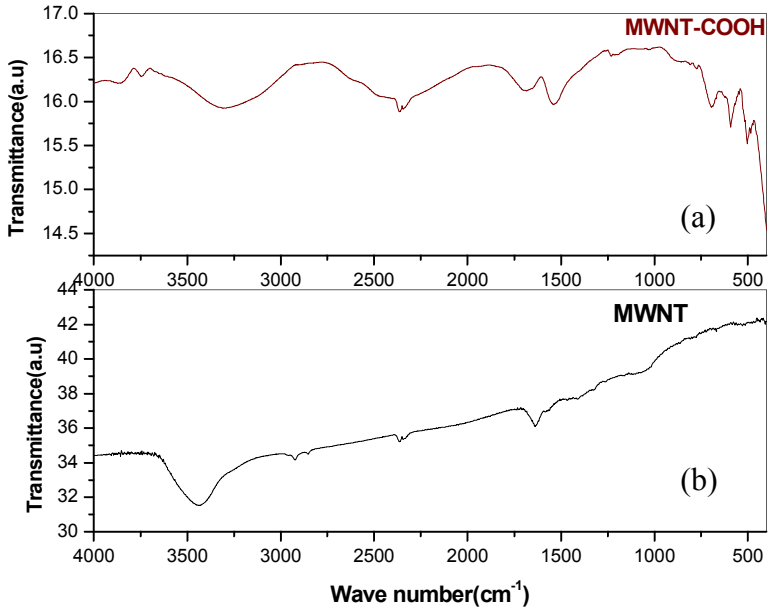

Figure 3.8 FTIR spectra of MWCNT; (a) Functionalised MWCNTs; (b) Pure MWCNTs

3.4.2 FTIR spectra of PVDF-MWCNTs composite

The FTIR spectrum of PVDF-MWCNTs composite is shown in figure 3.9. The peak observed at 508cm^{-1} corresponds to β-phase. The peak shifting observed in the region 838.72 cm^{-1} to 842.01cm^{-1} on addition of MWCNTs in PVDF matrix indicate suppression of α-phase and enhancement in β-phase. Broad peak observed at 1711.63 cm^{-1} and 1699.17cm^{-1} gives information about presence of carbonyl group and carboxylic group respectively due to addition of functionalized MWCNTs in PVDF matrix.

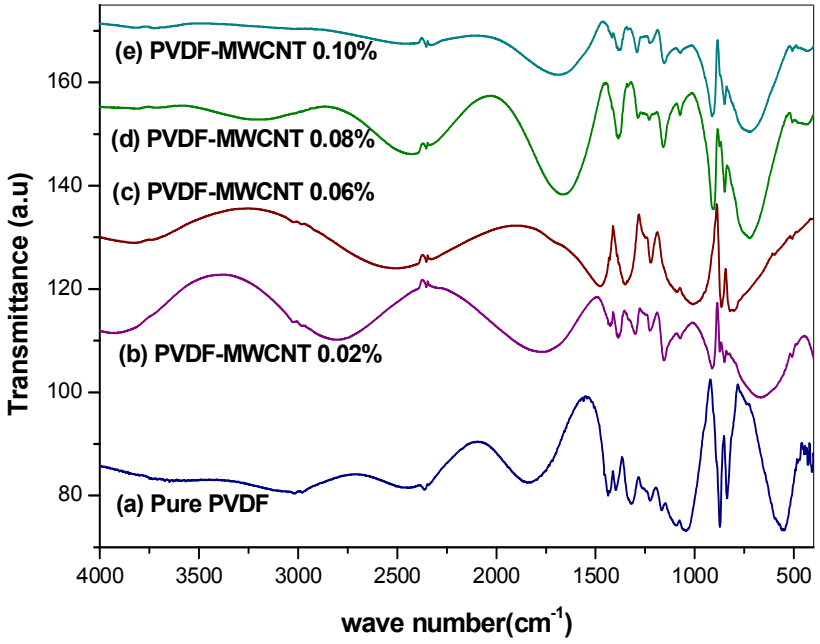

Figure 3.9 FTIR spectra of PVDF-MWCNTs composite films at different concentrations casting from the solution with 5:5 (THF/DMF) mass ratio; (a) Pure PVDF; (b) 0.02%; (c) 0.06%; (d) 0.08%; (e) 0.10% MWCNTs wt% respectively.

3.4.3 Structural analysis of PVDF-MWCNT composite

Figure 3.10 shows the XRD pattern of the MWCNTs doped PVDF film. The peaks with higher intensity extended over 2θ range revels the crystallinity of the doped sample. The peaks observed at 2θ = 19.28^{o}, 19.64^{o} and 19.24^{o} corresponds to α-phase and peaks observed at 2θ = 20.16^{o}, 20.14^{o} and 20.44^{o} shows presence of β–phase. It was observed that dispersion of MWCNTs does not affect the crystalline structure of PVDF.

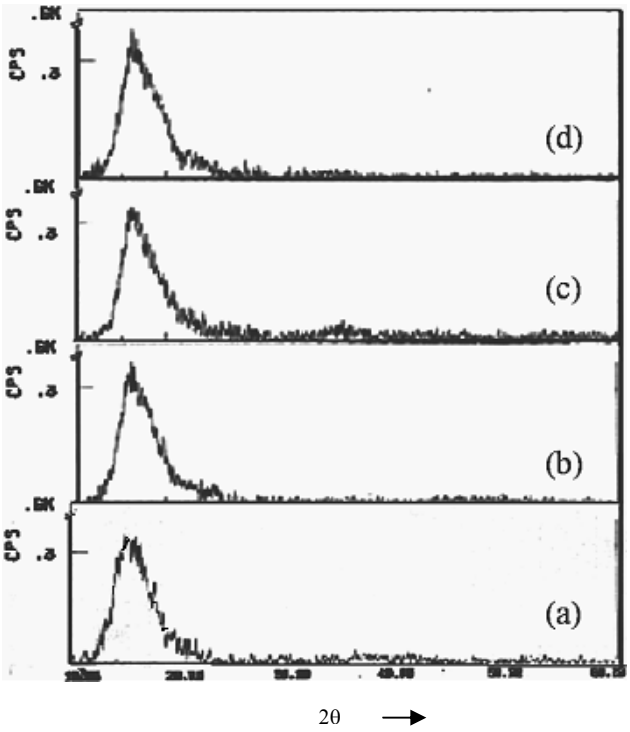

Figure3.10 X-ray pattern of PVDF-MWCNTs composite system at different concentrations of MWCNT in PVDF: a) 0.02%; b) 0.06%; c) 0.08%; d) 0.10% MWCNTs wt%.

3.5 Synthesis of PVDF-SiO_2 composite

3.5.1 FTIR spectra of functionalized silica nano-particle by Carboxylic group

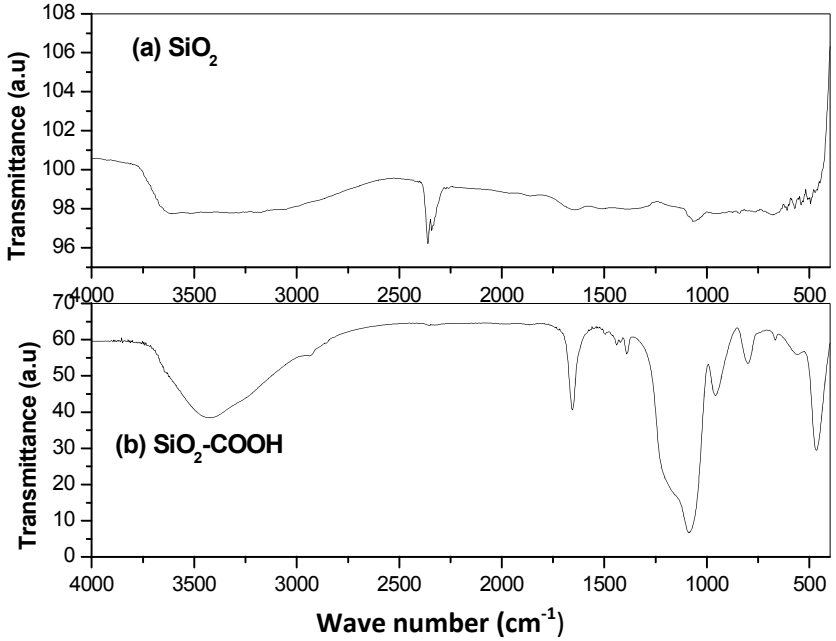

Figure 3.11 FTIR spectra of silica nano particle; (a) pure silica nano particle; (b) Functionalised silica nano particle.

FTIR spectrum of pure and functionalised silica nano particle is shown fig 3.11. In figure 3.11(a), the broad transmission peak between 3000-3500 cm^{-1} corresponds to OH bond which appears due to the absorbance of little moisture to the nanoparticles. Peak at 473 cm^{-1} and 1110 cm^{-1} observed due to the symmetric and asymmetric stretching vibration of Si–O–Si. In spectrum 3.11(b) the strong stretch at 3432 cm^{-1} corresponds to the OH group due to carboxylic acid. The strong broad peak observed in the region 1000 cm^{-1} to 1250 cm^{-1} due to Si–O–Si asymmetric stretching and C-O stretching of COOH acid.

3.5.2 Chemical analysis PVDF-SiO_2 composite

The FTIR spectra of PVDF-SiO_2 composite thin films are shown in figure3.12**.** In pure PVDF system peak observed at 598.35cm^{-1} corresponds to β-phase and more broadening in peak was observed with increase the concentration of silica nano particles. Further peak observed in the region 840 cm^{-1} indicative of β-phase in SiO_2 dispersed composite systems.

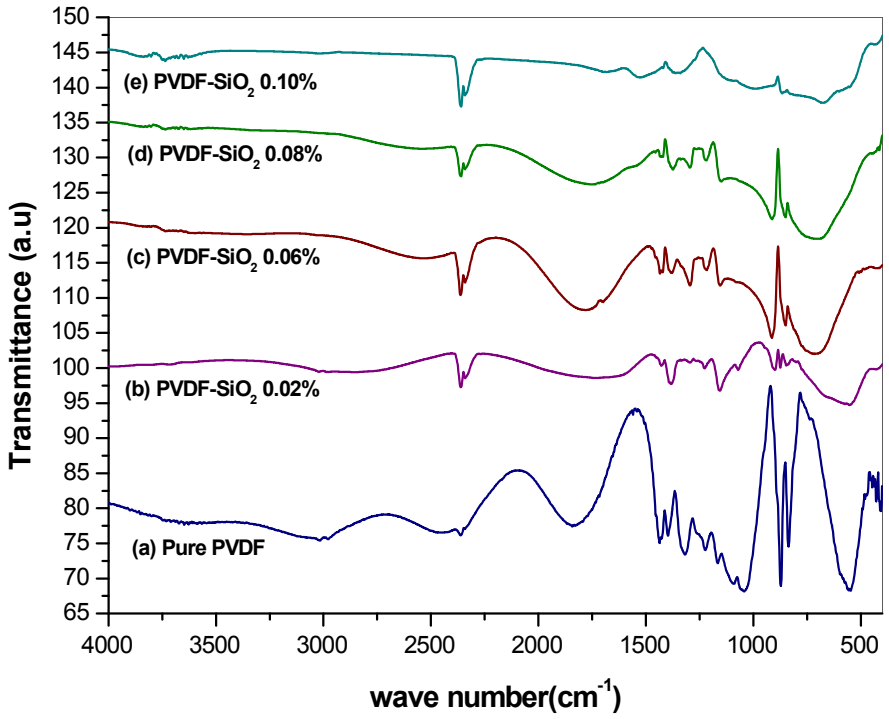

Figure 3.12 FTIR spectra of PVDF-SiO_2 composite films at different concentrations casting from the solution with 5:5 (THF/DMF) mass ratio. (a) Pure PVDF; (b) 0.02%; (c) 0.06%; (d) 0.08%; (e) 0.10% wt% SiO_2

3.5.3 Structural analysis of PVDF-SiO_2 composite

The XRD pattern of SiO_2 dispersed PVDF composite systems are shown in figure3.13. It is evident from the XRD pattern that the composite films are well crystalline. The peaks at 2θ =20.18^o and 20.48^o corresponds to β-phase moreover peaks at 2θ =18.26^o and 19.28^o corresponds to α-phase. We observed that with increasing concentration of SiO_2 particles the β-phase got suppressed α-phase become dominant.

.

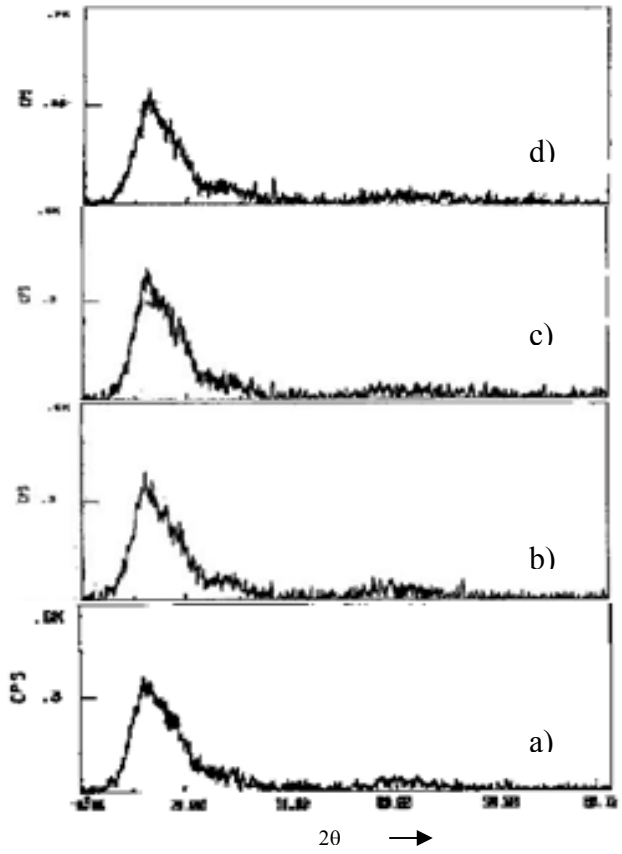

Figure3.13 X-ray patterns of PVDF-Silica (nano particle) composite system at different concentrations of: (a) 0.02; (b) 0.06; (c) 0.08; (d) 0.010 wt% SiO_2

3.6 Dielectric spectroscopy

The temperature and frequency dependent dielectric behaviour of thin film and bulk samples of MWCNTs and SiO_2 dispersed PVDF in the frequency range 50Hz to 1MHz and temperature range 25^{o}C to 200^{o}C has been studied.

3.6.1 Dielectric study of PVDF-MWCNT composite (Thin Film)

3.6.1.2 Frequency and temperature dependence of relative permittivity (ε′)

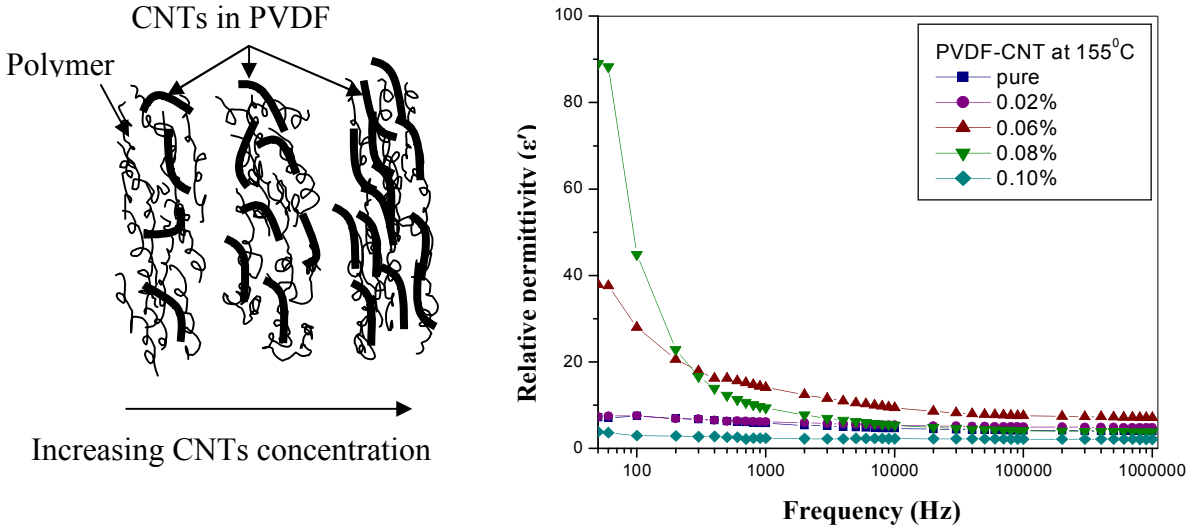

Figure 3.14 Variation of relative permittivity as a function of frequency at different concentrations of CNTs in PVDF.

The relative permittivity as a function of frequency at different concentration of MWCNTs is shown in figure 3.14. It was observed that the dielectric properties of the PVDF improved by adding MWCNTs in it. It was evident from the figure 3.14 that with increasing the concentration of MWCNTs, the dielectric constant gradually increase and attain maxima (89) at concentration 0.08 wt % in the lower frequencies region. With further increase in the frequency, the dielectric constant decreases sharply to lower value and attain saturation at higher frequencies region.

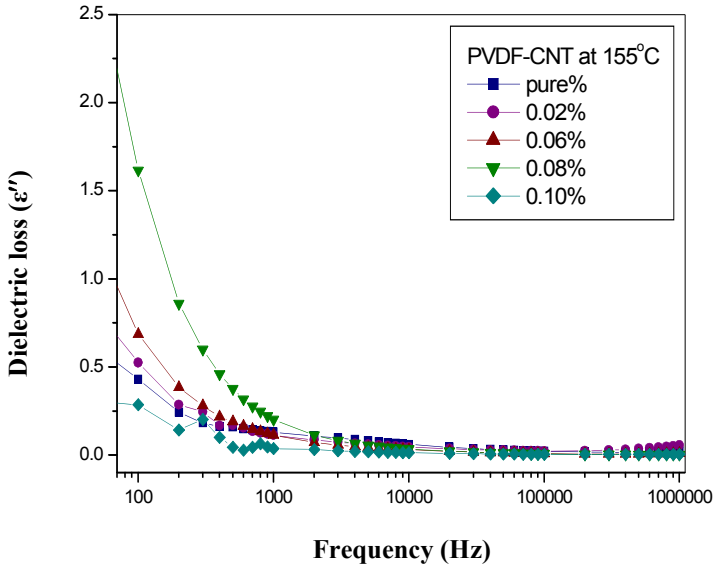

Figure 3.15 Variation of dielectric loss with frequency at different concentrations of CNT in PVDF.

The variation of dielectric loss of pure PVDF and MWCNTs dispersed thin films are shown in figure 3.15.We observed that at lower frequencies, the dielectric loss increased with increasing concentration of MWCNTs upto 0.08wt%.Whereas abrupt decrease in dielectric loss was observed at higher concentration (0.1wt%). At higher frequencies there was no significant variation in dielectric loss.

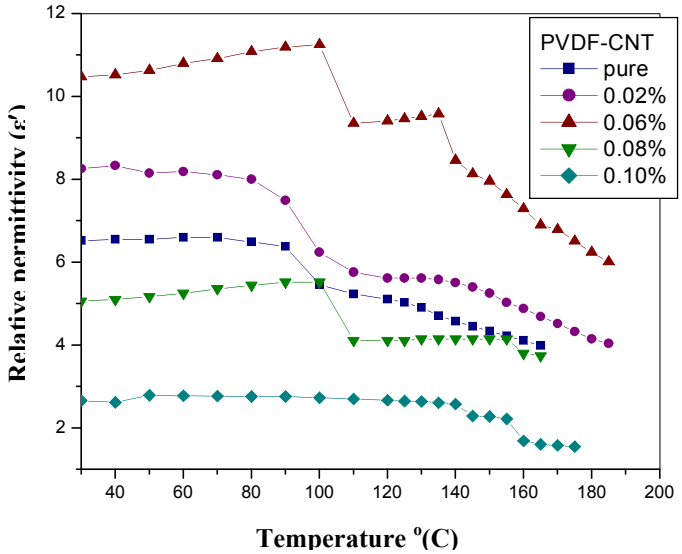

Figure 3.16 Variation of relative permittivity with temperature at different concentrations of CNT in PVDF at 100 kHz.

The variation in relative permittivity with temperature at different concentration of MWCNTs dispersed PVDF samples at 100 kHz are shown in figure 3.16. At 100 kHz, small increase in dielectric value was observed at 90^{o}C and then it decreases sharply up to 120^{o}C.The variation in dielectric permittivity in temperature region 90^{o}C to 120^{o}C occur due to phase transition from α to β-phase in PVDF. At higher temperature gradual decrease in relative permittivity was observed.

We believe that the high aspect ratio of MWCNTs increase the permittivity value of the composite system. The high aspect ratio of CNT surface has more zig-zag carbon atom which matches with all the trans conformation of β-phase also helps to increase crystallinity of β-phase. Also increase in dielectric behaviour of PVDF/MWCNTs composite system occurred due to change of α-phase percentage and interfacial polarization between PVDF and MWCNTs resulting from the MWCNTs entanglement. The increase in dielectric behaviour of PVDF/MWCNTs composite system can also be understood by mini-capacitor principle.

MWCNTs in PVDF can form a lot of mini-capacitors and their number increases with increase in MWCNTs concentration. The mini-capacitor may also form because of the COOH group on surface of MWCNTs. The isolation distance between MWCNTs decreases with increase in concentration so that the capacitance of mini capacitor increases.

3.6.2 Dielectric study of PVDF-SiO_2 composite (Thin Film)

3.6.2.1 Frequency and temperature dependence of relative permittivity (ε′)

The variation in relative permittivity as function of frequency for pure, SiO_2 dispersed PVDF samples are shown in figure 3.17. We observed that at lower concentrations, the relative permittivity of PVDF-Silica composite was not much influenced by doping of silica nano particles. As the amount of doping reached to 0.08 wt %, we found slight increase in dielectric permittivity (13) but at higher concentration (0.1wt %) it decreases sharply.

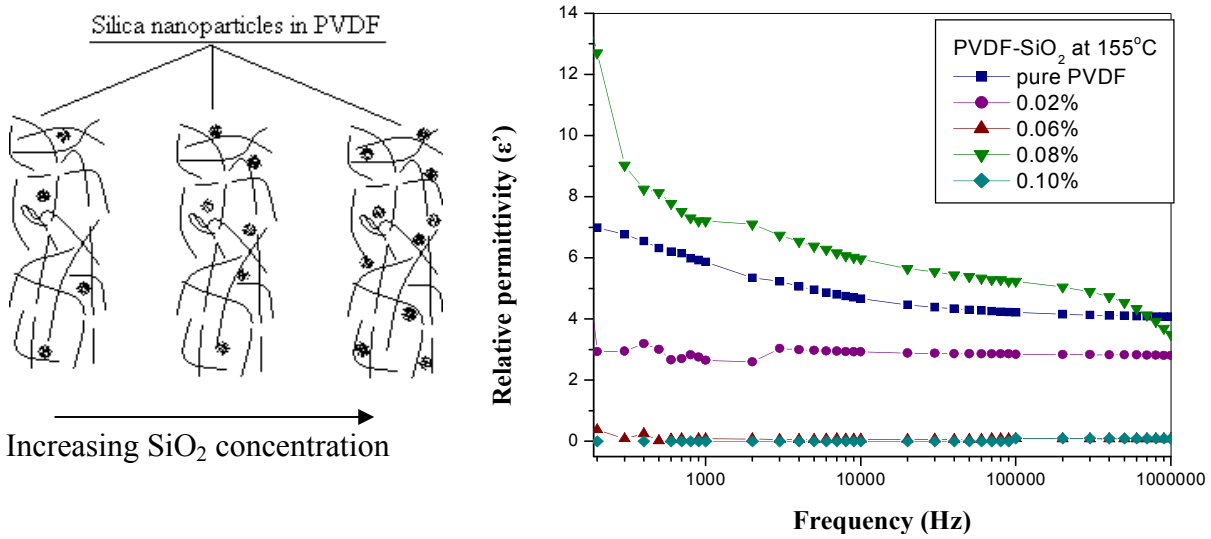

Figure 3.17 Variation of relative permittivity with frequency at different concentrations of Silica nanoparticles in PVDF.

The variation of losses in PVDF-SiO_2 composite w.r.t frequency at different concentration of SiO_2 nano particles are shown in figure 3.18. We observed that the dielectric losses in PVDF-SiO_2 composite system were lower as compare to pure PVDF system at lower concentrations in lower frequency region. The dielectric loss at concentrations 0.08 wt% was maximum and low at higher concentration. At higher frequencies we observed no significant change in the dielectric loss and they became constant.

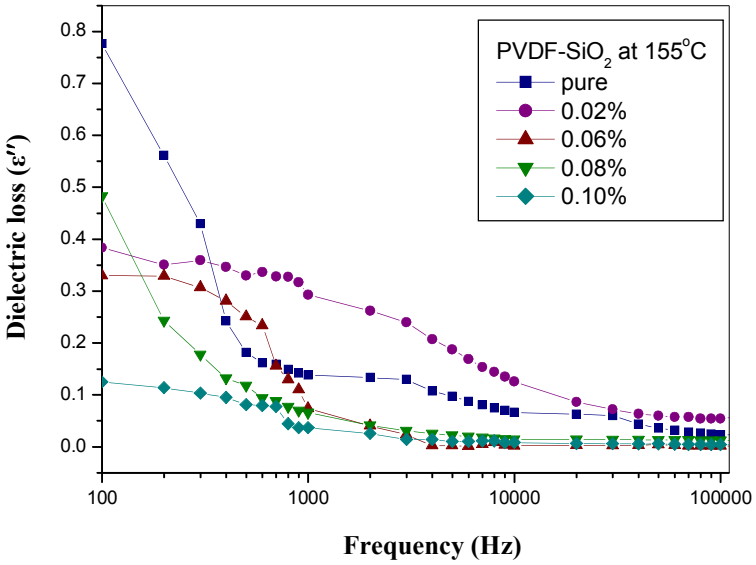

Figure 3.18 Variation of dielectric loss with frequency at different concentrations of SiO_2 in PVDF.

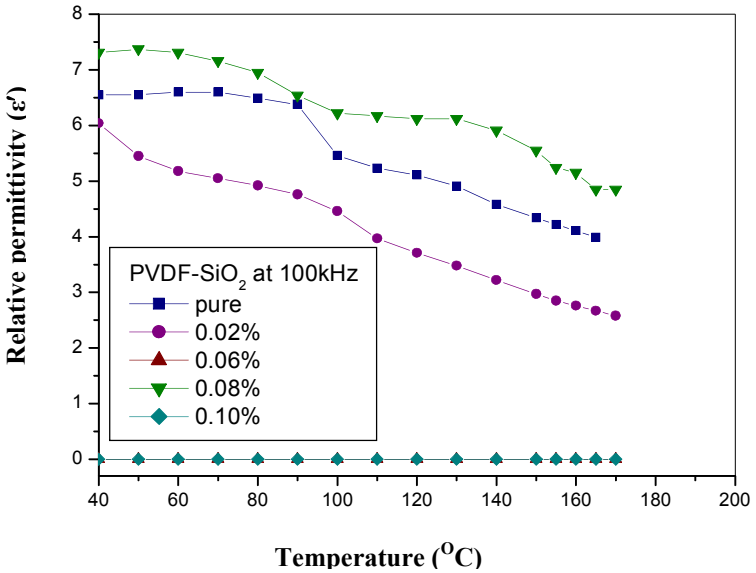

Figure 3.19 Variation of relative permittivity with temperature for different concentrations of SiO_2 in PVDF at 100 kHz.

Table3.1 Comparison of relative permittivity for thin film samples at different Concentration

Concentration (wt %)	Pure	0.02	0.06	0.08	0.1
Relative Permittivity of PVDF-MWCNT composite	7	9	39	89	5
Relative Permittivity of PVDF-SiO_2 composite	7	3.3	0.37	13	0.19

The variation in dielectric permittivity with temperature of pure and SiO_2 dispersed PVDF samples at 100 kHz are shown in figure 3.19. In temperature region 90°C to 120°C, rapid decrease in dielectric permittivity was observed, due to the phase transformation from α to β-phase. Further gradual decrease with increase in temperature was observed in all concentrations.

3.6.3 Dielectric study of PVDF-MWCNT composite (Bulk sample)

3.6.3.1 Frequency and temperature dependence of relative permittivity (ε′)

The relative permittivity variation as function of frequency for bulk samples is shown in figure 3.20. We observed that as the concentration of MWCNTs increased the relative permittivity shows gradual increase. The value of relative permittivity of bulk samples was found to be lower as compared to thin film samples.

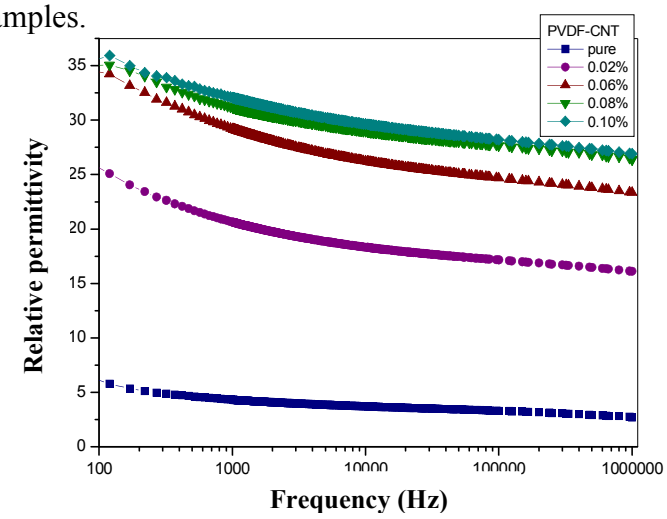

Figure 3.20 Variation of relative permittivity in bulk samples with frequency at different concentrations of CNT in PVDF.

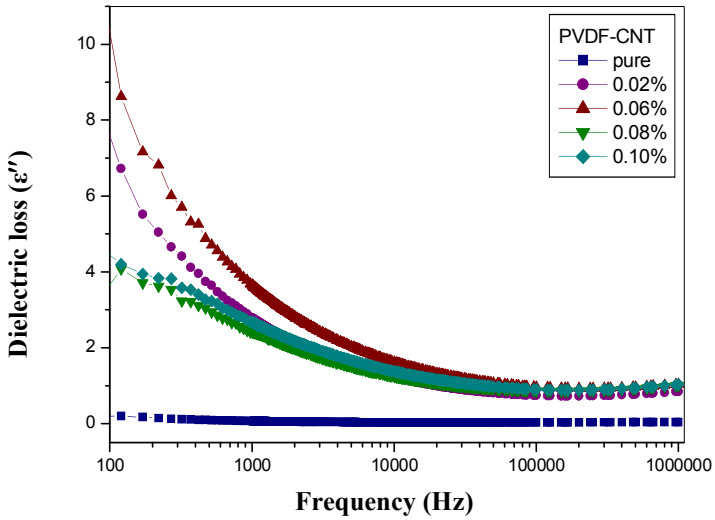

Figure 3.21 Variation of dielectric loss in bulk samples with frequency at different concentrations of CNT in PVDF.

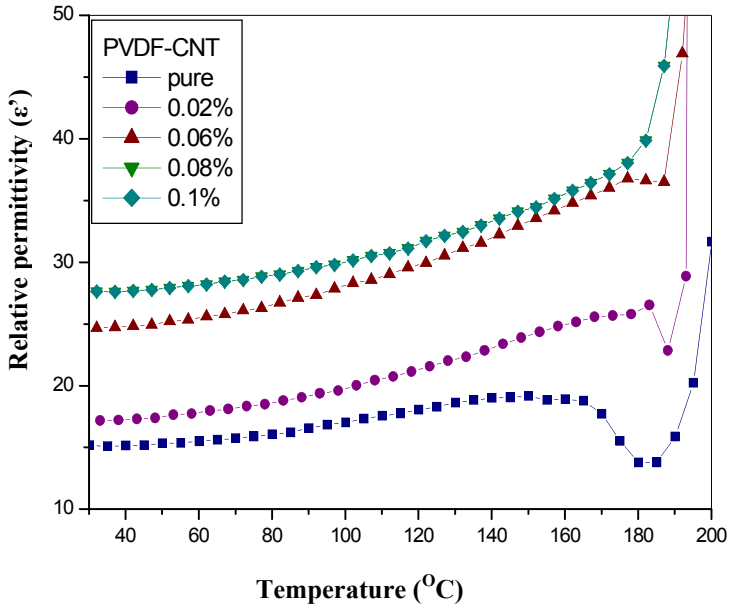

Figure 3.22 Variation of relative permittivity in bulk samples w.r.t temperature at different concentrations of CNT in PVDF.

Figure 3.21 shows that the dielectric loss in PVDF-MWCNTs bulk samples as function of frequency. We observed that the dielectric loss increases with increasing the concentration of MWCNTs and found to be higher as compare to losses in thin film samples.

The variation of dielectric permittivity with temperature at 100 kHz shown in figure3.22.It was observed that as the concentration of MWCNTs increased in PVDF matrix the transition temperature shifted towards higher value.

3.6.4 Dielectric study of PVDF-SiO_2 composite (Bulk sample)

3.6.4.1 Frequency and temperature dependence of relative permittivity (ε′)

Variation of dielectric permittivity with frequency at different concentrations of SiO_2 in PVDF bulk sample is shown in figure 3.23. It is evident from the figure that the value of relative permittivity increased with increasing concentration up to 0.06wt% and decline at higher concentrations (0.1wt %) of silica nanoparticles. We observed that dielectric permittivity of the SiO_2 doped samples was found to be higher as compare to thin film samples.

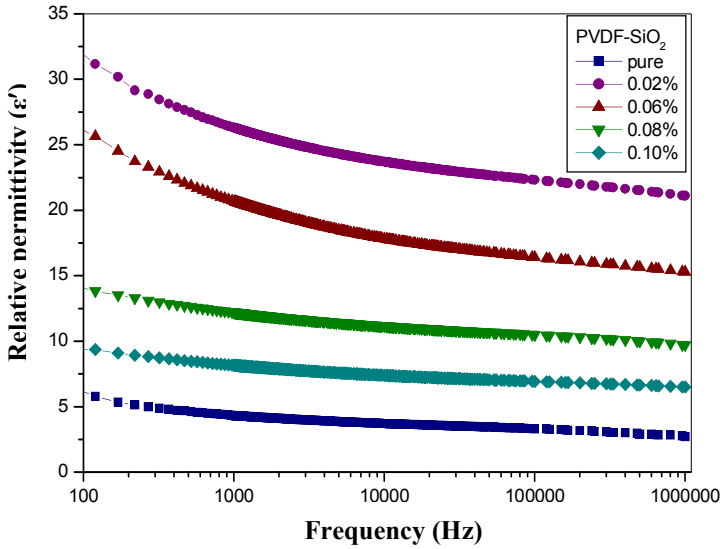

Figure 3.23 Variation of relative permittivity in bulk samples with frequency at different concentrations of SiO_2 in PVDF.

Figure 3.24 shows variation of dielectric loss for bulk samples of PVDF-SiO_2 composites system as a function frequency. We observed that dielectric losses were more at lower concentrations of SiO_2 and then gradually decreases with increase in concentration and became minimum at higher concentration (0.1 wt %).

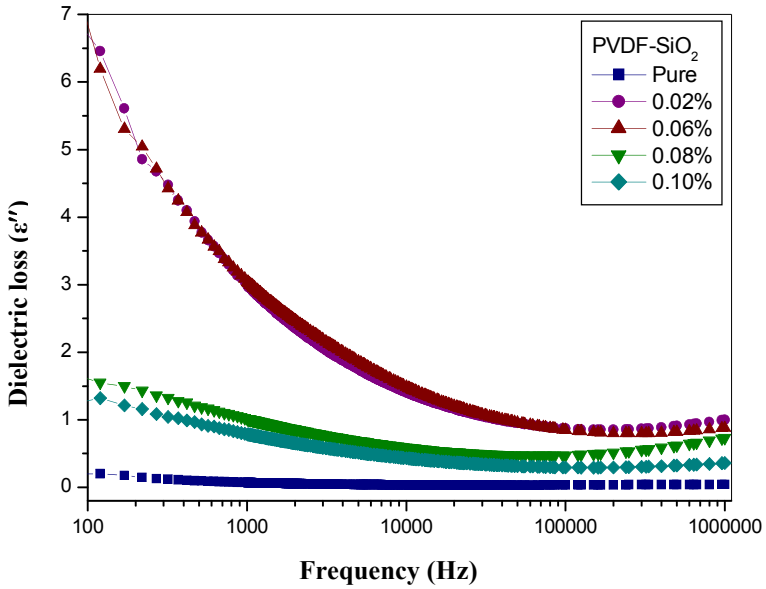

Figure 3.24 Variation of relative permittivity in bulk samples with frequency at different concentrations of SiO_2 .

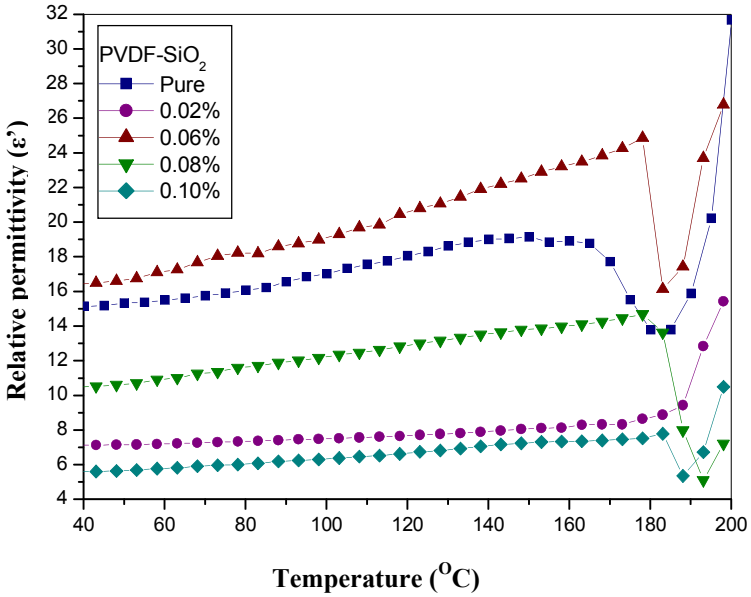

Figure 3.25 Variation of relative permittivity as function of temperature at 100 kHz for PVDF -SiO_2 composite bulk samples.

The figure 3.25 shows variation in relative permittivity as function of temperature at 100 kHz. At higher temperature, abrupt variation in relative permittivity was observed in the temperature region of 160°C to 200°C. The shift in transition temperature in PVDF-SiO_2 composites increases as the concentration of dopant was increased. The transition temperature of PVDF was 165.1°C and was shifted to 183°C at higher concentration (0.1 wt %) of silica nano particle.

Table3.2 Comparison of relative permittivity for bulk samples at different concentration

Concentration (wt %)	Pure	0.02	0.06	0.08	0.1
Relative Permittivity of PVDF-MWCNT composite	6	25	34	35	36
Relative Permittivity of PVDF- SiO_2 composite	6	32	25.80	14	9.18

Conclusion:

1) We prepared successfully β-phase of PVDF polymer via mixed solvent approach by optimizing the THF/DMF ratio 5:5. The synthesized pure PVDF thin film and nanoparticles doped PVDF films were amorphous as prepared and got crystallized with annealing at 90^{o}C (5h). We conclude that temperature plays an important role to achieve the crystallinity in such polymeric systems, and the formation of different phases strongly depends upon the temperature gradient as evident from structural and chemical analysis.
2) Morphological studied shows that the dispersed particles are homogeneously distributed in the PVDF matrix however some void spaces are seen in SiO_2 dispersed bulk system.
3) Carbon nanotubes dispersed in PVDF were homogeneously distributed in the polymer matrix and entangled with long chain of polymer without disturbing the crystalline structure of β-phase as evident from the XRD analysis. However the dispersion of SiO_2 suppress the β-phase and enhance the α-phase.
4) From chemical analysis (FTIR) we conclude that the addition of nanoparticles particularly MWCNTs enhance the β-phase as evident from FTIR spectra. However with the addition of SiO_2, β-phase got distorted at higher concentrations.
5) The relative permittivity for MWCNTs doped composite films increases up to 0.08 wt%, attains maxima at 89 and then decline at higher concentrations. The relative permittivity increases by 12 times from pure PVDF. However in the case of bulk samples, it gradually increases up to 0.1wt% concentration but the magnitude was found to be less (36).
6) The relative permittivity of SiO_2 doped composite film shows maximum value (13) at 0.08 wt% and having less value at lower and higher concentrations. In bulk samples, the relative permittivity was higher at lower concentrations and then decline with further increase in concentrations of SiO_2.
7) From dielectric investigation of PVDF composite system doped with different nanoparticles, we conclude that MWCNTs served as best dopant material as compared to the SiO_2. As our results shows the enhancement in relative permittivity in the MWCNTs doped system, which may be due to the capacitance principle in MWCNTs. The

MWCNTs works as mini-capacitors in the PVDF film and thus enhance relative permittivity.

Bibliography:

[1] Ajayan, P. M.; Braun, P. V.; Schadler, L. S.; "Nanocomposite science antechnology″; Wiley-VCH: Weinheim, (2003).

[2] Glushanin, S.; Topolov, V. Y.; Krivoruchko, A. V.; "Features of piezoelectric properties of 0-3 PbTiO3-type ceramic/polymer composites", *Materials Chemistry and Physics* 97 (2-3), 357-364, (2006).

[3] Hine, P.; Broome, V.; Ward, I.; "The incorporation of carbon nanofibres to enhance the properties of self reinforced, single polymer composites", *Polymer* 46 (24), 10936-10944, (2005).

[4] Cioffi, N.; Torsi, L.; Ditaranto, N.; Tantillo, G.; Ghibelli, L.; Sabbatini, L.; Bleve-Zacheo, T.; D'Alessio, M.; Zambonin, P. G.; Traversa, E.; "Copper nanoparticle/polymer composites with antifungal and bacteriostatic properties", *Chemistry of Materials* 17 (21), 5255-5262, (2005).

[5] Pelaiz-Barranco, A.; Marin-Franch, P.; "Piezo-, pyro-, ferro-, and dielectric properties of ceramic/polymer composites obtained from two modifications of lead titanate", *Journal of Applied Physics* 97 (3) (2005).

[6] Huang, Z. M.; Zhang, Y. Z.; Kotaki, M.; Ramakrishna, S.; "A review on polymer nanofibers by electrospinning and their applications in nanocomposites", *Composites Science and Technology* 63 (15), 2223-2253, (2003).

[7] Wilk G.D., R.M. Wallace & J.M. Anthony, Electrical Properties of Hafnium Silicate Gate Dielectrics Deposited Directly on Silicon. J. Appl. Phys. 89, 5243, (2001).

[8] Kingon A.I., J.P. Maria & S.K. Streiffer, Alternative Dielectric to Silicon Dioxide for Memory and Logic Device. Nature 406, 1032, (2000).

[9] Wenzhong Ma Æ Jun Zhang Æ Xiaolin Wang, J Mater Sci 43:398–401. (2008).

[10] The piezoelectricity of PVDF. Jpn J App Phys, 8 pp 975-976

[11] M. G. and Davis, G. T. 'Physical basis for piezoelectricity in PVDF', Ferroelectrics, 60:1, 3 - 13, (1984).

[12] Iijima, S.; "Helical Microtubules of Graphitic Carbon", *Nature* 354 (6348), 56-58, (1991).

[13] O'Connell, M. J.; "Carbon nanotubes properties and applications"; CRC Taylor & Francis: Boca Raton, (2006)

[14] Kataura, H.; Kumazawa, Y.; Maniwa, Y.; Umezu, I.; Suzuki, S.; Ohtsuka, Y.; Achiba, Y.; "Optical properties of multi-wall carbon nanotubes", *Synthetic Metals* 103 (1-3), 2555-2558, (1999).

[15] Wu, H. L.; Ma, C. C. M.; Yang, Y. T.; Kuan, H. C.; Yang, C. C.; Chiang, C. L.; "Morphology, electrical resistance, electromagnetic interference shielding and mechanical properties of functionalized MWNT and poly(urea urethane) nanocomposites", *Journal of Polymer Science Part B-Polymer Physics* 44 (7), 1096-1105, (2006)

[16] Hirsch, A.; Vostrowsky, O.; "Functionalization of carbon nanotubes", *Functional Molecular Nanostructures* 245, 193-237, (2005).

[17] Zhang, H. T.; Wu, G.; Chen, X. H.; Qiu, X. G.; "Synthesis and magnetic properties of nickel nanocrystals", *Materials Research Bulletin* 41 (3), 495-501, (2006).

[18] LizMarzan, L. M.; Giersig, M.; Mulvaney, P.; "Synthesis of nanosized gold-silica core-shell particles", *Langmuir* 12 (18), 4329-4335, (1996).

[19] Iijima, S.; Brabec, C.; Maiti, A.; Bernholc, J.; "Structural flexibility of carbon nanotubes", *Journal of Chemical Physics* 104 (5), 2089-2092, (1996).

[20] Chae, H. G.; Sreekumar, T. V.; Uchida, T.; Kumar, S.; "A comparison of reinforcement efficiency of various types of carbon nanotubes in poly acrylonitrile fiber", *Polymer* 46 (24), 10925-10935, (2005).

[21] Lau, K. T.; Hui, D.; "The revolutionary creation of new advanced materials - carbon nanotube composites", *Composites Part B-Engineering* 33 (4), 263-277, (2002).

[22] Odom, T. W.; Huang, J. L.; Kim, P.; Lieber, C. M.; "Atomic structure and electronic properties of single-walled carbon nanotubes", *Nature* 391 (6662), 62-64, (1998).

[24] Berger, C.; Poncharal, P.; Yi, Y.; de Heer, W.; "Ballistic conduction in multiwalled carbon nanotubes", *Journal of Nanoscience and Nanotechnology* 3 (1-2), 171-177, (2003).

[25] Urbina, A.; Echeverria, I.; Perez-Garrido, A.; az-Sanchez, A.; Abellan, J.; "Quantum conductance steps in solutions of multiwalled carbon nanotubes", *Physical Review Letters* 90 (10) (2003).

[26] Poncharal, P.; Berger, C.; Yi, Y.; Wang, Z. L.; de Heer, W. A.; "Room temperature ballistic conduction in carbon nanotubes", *Journal of Physical Chemistry B* 106 (47), 12104-12118, (2002).

[27] Schonenberger, C.; Bachtold, A.; Strunk, C.; Salvetat, J. P.; Forro, L.; "Interference and Interaction in multi-wall carbon nanotubes", *Applied Physics A-Materials Science & Processing* 69 (3), 283- 295, (1999).

[28] Minami, N.; Kazaoui, S.; Jacquemin, R.; Yamawaki, H.; Aoki, K.; Kataura, H.; Achiba, Y.; "Optical properties of semiconducting and metallic single wall carbon nanotubes: effects of doping and high pressure", *Synthetic Metals* 116 (1-3), 405-409, (2001).

[29] Banerjee, S.; Kahn, M. G. C.; Wong, S. S.; "Rational chemical strategies for carbon nanotube functionalization", *Chemistry-A European Journal* 9 (9), 1899-1908, (2003).

[30] Kim, J. A.; Seong, D. G.; Kang, T. J.; Youn, J. R.; "Effects of surface modification on rheological and mechanical properties of CNT/epoxy composites", *Carbon* 44 (10), 1898-1905, (2006).

[31] Park, H.; Zhao, J. J.; Lu, J. P.; "Effects of sidewall functionalization on conducting properties of single wall carbon nanotubes", *Nano Letters* 6 (5), 916-919, (2006).

[32] Dettlaff-Weglikowska, U.; Skakalova, V.; Graupner, R.; Jhang, S. H.; Kim, B. H.; Lee, H. J.; Ley, L.; Park, Y. W.; Berber, S.; Tomanek, D.; Roth, S.; "Effect of $SOCl_2$ treatment on electrical and mechanical properties of single-wall carbon nanotube networks", *Journal of the American Chemical Society* 127 (14), 5125-5131, (2005).

[33] Chen M., L. Wu, S. Zhou & B. You,. Synthesis of Rapsberry-like PMMA/SiO2 Nanocomposite Particles via a Surfactant-free Method. Macromolecules 37, 9613, (2004).

[34] Nalwa H.S. ed., Handbook of Organic–Inorganic Hybrid Materials and Nanocomposites, Chapter H-Conducting Polymer Nanocomposites, R. Gangopadhyay and A. De. (American Scientific Publishers), (2003).

[35] Roma G. & Y. Limoge, Density Functional Theory Investigation of Native Defects in SiO2: Self-Doping and Contribution to Ionic Conductivity. Phys. Rev. B 70, 174101, (2004).

[36] Campone P., M. Magliocco, G. Spinolo & A. Vedda,. Ionic Transport in Crystalline SiO2: The Role of Alkalimetals Ions and Hydrogen Impurities. Phys. Rev. B 52, 15903 (1995).

[37] Musikin S., L. Bakueva, E.H. Sargent & A. Sihk,. Luminescent Properties and Electronic Structure of Conjugated Polymer–Dielectric Nanocrystal Composites. J. Appl. Phys. 91, 6679 (2002).

[38] Bechinger, C.; Rudhardt, D.; Leiderer, P.; Roth, R.; Dietrich, S.; "Understanding depletion forces beyond entropy", *Physical Review Letters* 83 (19), 3960-3963, (1999).

[39] Meyyappan, M.; "Carbon nanotubes science and applications″; CRC Press: Boca Raton, FL, (2005).

[40] Hirsch, A.; Vostrowsky, O.; "Functionalization of carbon nanotubes", *Functional Molecular Nanostructures*245, 193-237, (2005).

[41] Baskaran, D.; Mays, J. W.; Bratcher, M. S.; "Polymer adsorption in the grafting reactions of hydroxyl terminal polymers with multi walled carbon nanotubes", *Polymer* 46 (14), 5050-5057, (2005).

[42] Ravindran, S.; Chaudhary, S.; Colburn, B.; Ozkan, M.; Ozkan, C. S.; "Covalent coupling of quantum dots to multiwalled carbon nanotubes for electronic device applications", *Nano Letters* 3 (4), 447-453, (2003).

[43] Fothergill J. C., Dissado L. A. (eds.): *Space Charge in Solid Dielectrics*, The Dielectrics Society, ISBN: 0 9533538 0 X, (1998).

[44] Fothergill J. C., Dissado L. A., *Electrical Degradation and Breakdown in Polymers*, IET Publisher,(1992).

[45] Mizutani T., Semi H., Kaneko K., 'Space charge behaviour in low-density polyethylene', *IEEE Transactions on Dielectrics and Electrical Insulation*, Vol: 7, No.: 4, pp 503–508, Aug (2000).

[46] Steven Boggs, 'A rational consideration of space charge', *DEIS*, Vol. 20, No. 4, July/August (2004).

[47] Montanari G. C., Mazzanti G., Palmieri F., Perego G., Serra S., 'Dependence of space-charge trapping threshold on temperature in polymeric DC cables,' in *Proc.2001 IEEE Int. Conf. Solid Dielect.,* pp. 81–84, (2001).

[48] Montanari G. C., 'Relation between space charge and polymeric insulation ageing: cause and effect', *IEEE Proc.-Sci. Meas. Technol.*, Vol. 150, No. 2, March (2003).

[49] Bernasconi J., 'Conduction in anisotropic disorder systems: Effective-medium theory', *Physical Review B*: Vol 9, No. 10, (1974).

[49] Carbeck JD, Rutledge GC In: Hougham G, Cassidy PE, Johns K, Davidson T (eds) Fluoropolymers 2: properties. Plenum Press, New York, p 191 (1999).

[50] Broadhurst MG, Davis GT J Appl Phys 49:4992 (1978)

[51] Matsushige K, Nagata K, Imada S, Takemura T Polymer 21:1391, (1980).

[52] Ma WZ, Zhang J, Wang XL, Wang SM Appl Surf Sci 253:8377, (2007).

[53] Davis GT, McKinney JE, Broadhurst MG, Roth SC J Appl Phys 49:4998, (1978).

[54] Wenzhong Ma Æ Jun Zhang Æ Xiaolin Wang, J Mater Sci 43:398–401, (2008).

[55] Qun Li, Qingzhong Xue , Qingbin Zheng, Lanzhong Hao, Xili Gao, Materials Letters 62 4229–4231, (2008).

[56] Chen M., L. Wu, S. Zhou & B. You, Synthesis of Rapsberry-like PMMA/SiO2 Nanocomposite Particles via a Surfactant-free Method. Macromolecules 37, 9613, (2004).

[57] Zhi-Min Dang,* Lan Wang, Yi Yin, Qing Zhang, and Qing-Qua Lei, Adv.Mater.,19,852-857,(2007).

[58] Harmon, J. P., Clayton, L. M., Muisener, P.: US20067094367 (2006).

[59] Dupire, M., Michel, J.: US20016331265 (2001).

[60] Ajayan PM, Stephan O, Colliex C, Trauth D. Aligned Carbon Nanotube Arrays Formed by Cutting a Polymer Resin-Nanotube Composite. Science; 265: 1212-1214, (1994).